



UNIUNEA EUROPEANĂ



GUVERNUL ROMÂNIEI
MINISTERUL MUNCII, FAMILIEI,
PROTECȚIEI SOCIALE ȘI
PERSOANELOR VÂRSTNICE
AMPOSDRU



Fondul Social European
POSDRU 2007-2013



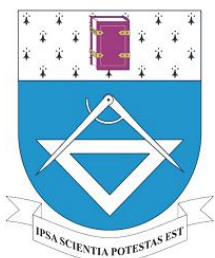
Instrumente Structurale
2007-2013



MINISTERUL
EDUCAȚIEI
NAȚIONALE
OIPOSDRU



UNIVERSITATEA TEHNICĂ
"GHEORGHE ASACHI" DIN
IASI



THE "GH. ASACHI" TECHNICAL
UNIVERSITY OF IAȘI
Faculty of Chemical Engineering and
Environmental Protection



NANOSTRUCTURED MATERIALS TYPE LAYERED DOUBLE HYDROXIDES (LDHs) WITH SPECIFIC PROPERTIES AND APPLICATIONS

- SUMMARY OF THE Ph.D. THESIS -

PhD Supervisor:
Prof. univ. dr. Gabriela Carja

PhD Student:
Eng. Mihaela Birsanu

IAȘI - 2013



UNIUNEA EUROPEANĂ



GUVERNUL ROMÂNIEI
MINISTERUL MUNCII, FAMILIEI,
PROTECȚIEI SOCIALE ȘI
PERSOANELOR VÂRSTNICE
AMPOSDRU



Fondul Social European
POSDRU 2007-2013



Instrumente Structurale
2007-2013



MINISTERUL
EDUCAȚIEI
NAȚIONALE
OIPOSDRU



UNIVERSITATEA TEHNICĂ
"GHEORGHE ASACHI" DIN
IASI

Teza de doctorat a fost realizată cu sprijinul financiar al proiectului
**“STUDII DOCTORALE PENTRU PERFORMANȚE EUROPENE ÎN CERCETARE ȘI
INOVARE (CUANTUMDOC)”** POSDRU/107/1.5/S/79407.

Proiectul **“STUDII DOCTORALE PENTRU PERFORMANȚE EUROPENE ÎN
CERCETARE ȘI INOVARE (CUANTUMDOC)”** POSDRU/107/1.5/S/79407, este un
proiect strategic care are ca obiectiv general *„Aplicarea de strategii
manageriale, de cercetare și didactice destinate îmbunătățirii formării inițiale
a viitorilor cercetători prin programul de studii universitare de doctorat,
conform procesului de la Bologna, prin dezvoltarea unor competențe
specifice cercetării științifice, dar și a unor competențe generale:
managementul cercetării, competențe lingvistice și de comunicare, abilități de
documentare, redactare, publicare și comunicare științifică, utilizarea
mijloacelor moderne oferite de TIC, spiritul antreprenorial de transfer al
rezultatelor cercetării. Dezvoltarea capitalului uman pentru cercetare și
inovare va contribui pe termen lung la formarea doctoranzilor la nivel
european cu preocupări interdisciplinare. Sprijinul financiar oferit
doctoranzilor va asigura participarea la programe doctorale în țara și la stagii
de cercetare în centre de cercetare sau universități din UE. Misiunea
proiectului este formarea unui tânăr cercetător adaptat economiei de piață și
noilor tehnologii, având cunoștințe teoretice, practice, economice și
manageriale la nivel internațional, ce va promova principiile dezvoltării
durabile și de protecție a mediului înconjurător.”*

Proiect finanțat în perioada 2010 - 2013

Finanțare proiect: **16.810.100,00** RON

Beneficiar: Universitatea Tehnică “Gheorghe Asachi” din Iași

Partener: Universitatea „Babeș Bolyai” din Cluj-Napoca

Director proiect: Prof. univ. dr. ing. Mihai BUDESCU

Responsabil proiect partener: Prof. univ. dr. ing. Alexandru OZUNU

UNIVERSITATEA TEHNICĂ "GHEORGHE ASACHI" DIN IAȘI
R E C T O R A T U L

Către

Vă facem cunoscut că, în ziua de **28 noiembrie**, la ora **11⁰⁰** în Sala de Consiliu a Facultății de Inginerie Chimică și Protecția Mediului, va avea loc susținerea publică a tezei de doctorat intitulată:

**"MATERIALE NANOSTRUCTURATE DE TIP HIDROXIZI DUBLU LAMELARI (LDHs)
CU PROPRIETĂȚI ȘI APLICAȚII SPECIFICE"**

elaborată de doamna **ing. Bîrsanu Mihaela** în vederea conferirii titlului științific de doctor în Inginerie Chimică.

Comisia de doctorat este alcătuită din:

- | | |
|--|------------------------|
| 1. Prof. univ. dr. ing. Silvia Curteanu
Universitatea Tehnică „Gheorghe Asachi”, Iași | președinte |
| 2. Prof. univ. dr. ing. Gabriela Cârjă,
Universitatea Tehnică „Gheorghe Asachi”, Iași | conducător de doctorat |
| 3. Prof.univ.dr. chim. Hermenegildo Garcia Gomez
Universitatea Politehnică din Valencia | referent oficial |
| 4. Prof. univ. dr. Vanessa Prevot
Universitatea „Blaise Pascal”, Franța | referent oficial |
| 5. Prof. univ. dr. chim. Aurel Pui
Universitatea „Alexandru Ioan Cuza” , Iași | referent oficial |

Vă trimitem rezumatul tezei de doctorat cu rugămintea de a ne comunica, în scris, aprecierile dumneavoastră.

Cu această ocazie vă invităm să participați la susținerea publică a tezei de doctorat.


RECTOR,
Prof.univ.dr.ing. **ION GIURMA**

Secretar universitate,

Ing. Cristina Nagiț

TABLE OF CONTENTS

INTRODUCTION.....	4
 PART I. STATE OF THE ART IN THE FIELD	
I. Literature review on layered double hydroxides and their self-assemblies.....	16
I.1. Layered double hydroxides (LDHs): definition and structural properties.....	16
I.2. Fabrication methods of LDHs, Me/LDHs and Me_xO_y/LDHs nanostructures.....	21
I.2.1. Coprecipitation method.....	21
I.2.2. Ion-exchange method.....	24
I.2.3. Reconstruction method.....	25
I.2.4. Hydrothermal method.....	26
I.2.5. Urea hydrolysis method.....	27
I.2.6. Sol – gel method.....	28
I.3. Physical-chemical properties of LDHs, Me/LDHs and Me_xO_y/LDHs nanostructures.....	29
I.3.1. X-ray diffraction (XRD).....	29
I.3.2. Fourier transform infrared spectroscopy (FTIR)	34
I.3.3. Thermal analysis (TG/DTG/DTA).....	38
I.3.4. UV-Vis analysis.....	42
I.3.4. Scanning electron microscopy (SEM).....	45
I.3.5. Transmission electron microscopy (TEM).....	48
I.4. Layered double hydroxides (LDHs) and their derived mixed oxides: photoresponsive properties and photocatalytic applications.....	52

PART II. RESULTS OF THE EXPERIMENTAL RESEARCH ACTIVITY; ORIGINAL CONTRIBUTIONS

II. Fabrication and physical-chemical properties of LDHs precursors.....	60
II.1. Fabrications procedures of LDHs precursors	60
II.2. Physical-chemical characterization of the LDHs precursors.....	62
II.2.1. X-ray diffraction (XRD).....	62
II.2.2. Fourier transform infrared spectroscopy (FTIR).....	64
II.2.3. Thermal analysis (TG-DTG).....	65
II.2.4. Field emission scanning electron microscopy (FESEM).....	67
II.3. Conclusions.....	69
III. Preparation and characterization of the nanostructured assemblies based on LDHs.....	71
III.1. Fabrication of Au/LDHs nanostructured assemblies (Au/MgAlLDH, Au/ZnAlLDH, Au/ZnCeAlLDH).....	71
III.2. Physical-chemical characterization of Au/LDHs by XRD, FTIR, TG-DTG, TEM, FESEM analysis.....	72
III.3. Fabrication of Fe₂O₃/LDHs nanostructures (Fe₂O₃/MgAlLDH, Fe₂O₃/MgFeAlLDH, Fe₂O₃/ZnAlLDH).....	88
III.4. Physical-chemical characterization of Fe₂O₃/LDHs by XRD, FTIR, TG-DTG, TEM, SEM analysis.....	88
III.5. Conclusions.....	95
IV. Photocatalytic applications of LDHs, Me/LDHs, Me_xO_y/LDHs nanostructures and their derived mixed oxides.....	97
IV.1. Studies on Au/LDHs as novel photocatalysts for water splitting process.....	97

IV.2. Studies on Fe ₂ O ₃ /LDHs as novel photocatalysts for degrading industrial dyes (e.g. Drimaren Red and Nylosan Navy- Clarinte Productt).....	107
GENERAL CONCLUSIONS	115
SCIENTIFIC ACTIVITY	118
REFERENCES	121

The summary of the thesis presents introduction, parts of the results of experimental research, general conclusions and some references.

INTRODUCTION

Layered double hydroxides (LDHs) are cheap eco-friendly materials, which belong to the class of anionic clays. They have recently attracted a great deal of attention in many technological fields, such as catalysis, nanomedicine, separation and nanotechnology, due to their interesting properties in anion exchangeability, compositional flexibility and biocompatibility. LDHs materials are defined by a brucite-like structure; they are obtained from the isomorphic substitution of a part of the divalent cations with the trivalent cations in the brucite-like positively charged layers. The LDHs typical lamellar packing stability is achieved by the interlayer counter anions, as well as, by water molecules. The large variety of the compositions that can be developed by altering the nature of the divalent and trivalent cations in the layers, the type of interlayer anions and/or the stoichiometric coefficient might give rise to a large compositional diversity of LDH like-materials and specific textural properties. In terms of their texture, layered double hydroxides are composed of the self-organized patterns of large, interconnected nanoparticles assemblies. Constructing the LDHs based nanostructures implies not only to tailor the size and shape of the LDHs large nanoparticles but also to design the particles interconnection patterns for giving rise to tailored inter-particle nanosized spaces. Very recently, LDHs have also been used as specific building components in complex nanoassemblies. Nanoparticles of metal (Me) or metal oxides (Me_xO_y) received a high interest in the last decades due to their special properties within nano-range. Hence, their widely nano-applications have promoted the emergence of a new science: nanotechnology. One specific problem regarding nanoparticles of metal and/or metal oxides, that scientists have to cope, is their reduced stability within nanorange thus the preservation of their nano characteristics.

In this view, my Ph.D. research activities have been focused on the fabrication of LDHs and the derived nanostructured assemblies, type: Me/LDHs and Me_xO_y /LDHs. The physical-chemical properties of the obtained LDHs based nanorhitectonics and the **novel** photocatalytic applications of these materials have been also studied.

Our results indicate that the materials based on nanostructured LDHs and their assemblies, type Me/LDHs and Me_xO_y /LDHs can be obtained in a tailored compositional diversity that afford the design of valuable catalysts for the photocatalytic degradation process from aqueous solutions of some toxic organic compounds (type industrial dyes), as well as, **novel efficient photocatalysts for the process of water splitting under sun-light irradiation for the production of H_2 .**

The objectives of the research activity and the thesis structure:

The **MAIN OBJECTIVE** of the thesis has been to get new knowledge regarding the structural reconstruction process of the LDHs in the aqueous solutions, type Me^+X^- . This has been afforded us to further manipulate the fabrication procedures of Me/LDHs and/or $\text{Me}_x\text{O}_y\text{/LDHs}$ nanostructures based on the LDHs reconstruction process.

This structural reconstruction is based on a very specific and interesting property of the LDHs, so-called structural ‘memory effect’. This means that the layered clay structure, that can be destroyed by calcination at moderate temperatures (ca. 550°C) to yield low crystalline mixed oxides, can be reconstructed in aqueous solutions containing anionic species. Up to this moment it is clear for us that, during the LDHs reconstruction, the anions of the solutions will be taken to serve as interlayer anions of the LDH matrix though we have limited knowledge how the cations of the solutions are organized in the form of nanoparticles on the surface of the large nanoparticles of the LDHs. In this reason, the research activity was focused to deeply study of the LDHs reconstruction process in the aqueous solutions of gold salts ($\text{Au}^{y+}\text{X}^{3-}$)₃ and the aqueous solutions of iron salts ($\text{Fe}^{y+}\text{X}^{3-}$). Not only the different nature of the Me^+X^- ($\text{X} = \text{Cl}^-$, SO_4^{2-} , CH_3COO^-) aqueous solutions but also the tailored composition of the LDHs were used as the controlled variable (e.g. MgAlLDH , ZnAlLDH , FeLDH , ZnCeAlLDH) during the reconstruction process.

Specific objectives of the research included in the thesis:

- ❖ Studies regarding the manifestation of the structural memory effect of the LDHs in $\text{Au}^{y+}\text{X}^{3-}$ aqueous solutions by using LDHs with variable compositions (e.g.: MgAlLDH , ZnAlLDH , FeLDH , ZnCeAlLDH).
- ❖ Studies regarding the manifestation of the structural memory effect of the LDHs in $\text{Au}(\text{O}_2\text{CCH}_3)_3$, AuSO_4 , AuCl_3 aqueous solutions for tailoring the structural reconstruction of ZnAlLDH .
- ❖ Studies regarding the manifestation of the structural memory effect of the LDHs in $\text{Fe}^{y+}\text{X}^{3-}$ aqueous solutions by using LDHs with variable compositions (e.g.: MgAlLDH , ZnAlLDH , FeLDH).
- ❖ Studies on Au/LDHs and Fe/LDHs * nanoarchitectonics by FESEM and TEM analysis.
- ❖ Studies on the physical–chemical properties of Au/LDHs and Fe/LDHs nanoarchitectonics by using XRD analysis, FTIR analysis and XPS analysis.
- ❖ Studies on the photoresponsive properties of Au/LDHs and Fe/LDHs nanoarchitectonics by UVVis analysis. Studies on the plasmonic characteristics of AuNPs in Au/LDHs nanostructures.

* Note that $\text{Fe}_2\text{O}_3\text{/LDHs}$ is denoted in this work as Fe/LDHs

- ❖ Photocatalytic studies and tests: LDHs, Au/LDHs and the derived mixed oxides nanoarchitectonics as **novel** photocatalysts for **water splitting** (WSP), under solar irradiation.
- ❖ Photocatalytic studies and tests: LDHs, Fe/LDHs and the derived mixed oxides nanostructures as **novel** photocatalysts for the photocatalytic degradation of some industrial dyes offered by the CLARINTE PRODUCKT Company, Switzerland.

The structure of my Ph. D. thesis is:

- **Part I** – STATE OF THE ART IN THE FIELD of LDHs synthesis, properties and nanoarchitectonics.
- **Part II** - RESULTS OF THE EXPERIMENTAL RESEARCH ACTIVITY; ORIGINAL CONTRIBUTIONS which includes three chapters.

The first chapter summarizes general knowledge from literature about the structure, specific properties and the main synthesis methods of the LDHs. This chapter also treats the modern techniques of physical-chemical analysis of LDHs, such as examples of applications of the LDHs and LDHs nanostructures.

The second chapter introduces the results obtained in my research activity during Ph. D. studies. The chapter presents the final experimental protocol of LDHs anionic clay fabrication type ZnAILDH, ZnCeAILDH and MgFeAILDH, physico-chemical characteristics using analytical techniques: X-ray diffraction (XRD), Fourier transforms infrared spectroscopy (FTIR), thermogravimetric analysis (TG-DTG) and field emission scanning electron microscopy (FESEM).

Chapter three presents the fabrication process of nanoarchitectonics type metal nanoparticles deposited onto mesoporous LDHs matrices; the obtained nanoassemblies were: Au/ZnAILDH, Au/MgAILDH, Au/ZnCeAILDH as function of different nature of X^{3-} of Au salt solutions and $Fe_2O_3/MgAILDH$ and $Fe_2O_3/MgFeAILDH$. Aspects regarding the structural reconstruction process of the LDHs, their interlayer properties, the surface characteristics, their textural and morphological properties are deeply studied and discussed.

Chapter four points out the specific applications of LDHs, Me/LDHs and $Me_xO_y/LDHs$ nanoarchitectures like novel efficient photocatalysts. Regarding this, the first section describes the photocatalytic activity of gold nanoparticles deposited onto mesoporous LDHs matrices for the production of hydrogen from a mixed solution of water and methanol, using a solar radiation source. The photoresponsive properties of the precursor materials and Au/LDHs matrices nanostructured materials and their photocatalytic performances in water splitting process, are studied and discussed.

Further, the next section describes the photocatalytic degradation of the industrial dyes from aqueous solutions using MgAlLDH, MgFeAlLDH and Fe₂O₃/MgFeAlLDH photocatalysts. Moreover this part presents the obtained results regarding the photoresponsive properties of the nanostructured LDH- based catalysts, the band gap energy and the higher photocatalytic activity of Me_xO_y/LDHs nano-assemblies compared with the LDHs precursors.

The final part of the thesis consists of *General Conclusions* and *References*.

The results obtained from the research activity were disseminated by the publication of 2 articles in ISI journal, 2 articles prepared for the publication and also by the participation at 7 national and international conferences.

The novelty and originality of the research work

We obtained new knowledge regarding the reconstruction process of the LDHs (based on its structural memory effect) in the aqueous solutions of gold salts (Au^{y+}X³⁻) and the aqueous solutions of iron salts (Fe^{y+}X³⁻), giving rise to complex nanoarchitectonics described as nanoparticles of Au or Fe₂O₃ deposited on the larger nanoparticles of the LDHs. This procedure is performed in a single step at room temperature. Therefore, the conjugation of the intercalation process of anions with the adsorption process of cations - when an aqueous solution of metal salt is used during the clay structural reconstruction - gives rise to nanostructured ensembles of nanoparticles of Au or Fe₂O₃ deposited on the LDHs matrices. It is noteworthy that no organic compounds were used during the fabrication procedure of these, LDHs based nanoarchitectonics.

Further the results of physical-chemical analysis (by XRD, TEM, FESEM, XPS) reveal that these **novel nanostructured materials** are able to combine the properties of the porous matrix of the LDHs and the induced characteristics that are specific of the nanosized Au or Fe₂O₃ into one single material. The LDHs matrix is also able to bring into cumulative structure not only the advantage of a good biocompatibility and versatile composition but also the high adsorption capacities and controlled textural features within nano range, considering that the textural features are very important for tuning the characteristics of the physical-chemical processes occurring at active interfaces, in catalytic applications.

We studied, to our knowledge, for the first time, the self-assembly of Au nanoparticles/mesoporous matrices of layered double hydroxides (Au/ZnAlLDH and Au/ZnCeAlLDH) and the derived mixed oxides as **novel plasmonic photocatalysts** for H₂ production from water-methanol mixtures by using solar irradiation, at room temperature.

These results open new opportunities for progress in the development of plasmonic nanoarchitectonics for solar-light driven photocatalysts for clean H₂ production.

Furthermore, the photoresponsive properties of Fe/LDHs and the catalytic behavior of these novel materials in the process of UV photocatalytic degradation of Drimaren Red and Nylosan Navy have been studied.

Results demonstrated that the photoresponsive performances of Au/LDHs and Fe/LDHs (it is in fact Fe₂O₃ but in the thesis we denoted it as Fe/LDHs) are established by both the characteristics and nature of the supported nanoparticles and also by the characteristics of the LDHs.

The results of the thesis have been disseminated as follows:

Articles published in ISI journals

1. G. Carja, **M. Birsanu**, K. Okada, H. Garcia,
Composite plasmonic gold/layered double hydroxides and derived mixed oxides as novel photocatalysts for hydrogen generation under solar irradiation,
Journal of Materials Chemistry A, (RCS Publications) 2013, 1, 9092-9098
2. **M. Birsanu**, M. Puscasu, C. Gherasim, G. Carja,
Highly efficient room temperature degradation of two industrial dyes using hydrotalcite – like anionic clays and their derived mixed oxides as photocatalysts,
Environmental Engineering and Management Journal, 12 (2013), 5, 1535-1540
3. K. Katsumata, **M. Birsanu**, K. Ikeda, K. Okada, G. Carja,
Gold nanoparticles on layered double hydroxides: plasmonic versus electron charging effects for efficient aqueous CO₂ reduction at room temperature, manuscript under publication (2013).
4. **M. Birsanu**, G. Carja, H. Garcia,
Novel visible light responsive photocatalysts type LDHs and their derived mixed oxides for degradations of Methylene Blue, manuscript under preparation.

Articles included in CNCSIS journals

1. D. Mardare, **M. Birsanu**, G. Apostolescu, G. Carja,
Layered Double Hydroxides as Inorganic Versatile and Multifunctional Materials,
Bulletin of the Polytechnic Institute of Iasi, Department of Chemistry and Chemical Engineering, 2011, Tome LVII (LXI), **Fasc. 3, 43-62**, ISSN 0254-7104.

Articles included in Workshop volume

1. M. Birsanu,

Study of physic-chemical properties and morphology of LDHs nanostructures used in catalytic process, Workshop volume "Trends and requirements of interdisciplinarity in research", Iasi, 25 January, Doctoral Studies project for European Research and Innovation Performance CUANTUMDOC – POSDRU/107/1.5/S/7940725, 11-18.

Communications at national and international conferences

1. Laura Dartu, Sofronia Dranca, **Mihaela Birsanu**, Gabriela Carja, Nanoparticles of Zinc Oxide/Zinc Substituted Layered Double Hydroxides as Nanostructured Self – Assemblies, în cadrul conferinței „E-MRS 2011 FALL MEETING”, organized by University of Technology Warsaw, in the period 19-23 September 2011, Warsaw, Poland.

2. Dragoș Mardare, **Mihaela Birsanu**, Gabriela Apostolescu, Gabriela Carja, Layered Double Hydroxides as Inorganic Versatile and Multifunctional Materials, at the conference „Materials and processes innovative”, organized by Faculty of Chemical Engineering and Environmental protection”, VIII edition, during the period 17-18 November 2011, Iași, România.

3. Elena Husanu, Magda Puscasu, Livia Bibire, **Mihaela Birsanu**, Gabriela Carja, Uptake of As (V) From Aqueous Solution by mixed oxides derived from copper substituted layered double hydroxides, at International Conference on Monitoring of Water Pollution and Wastewater Treatment Technologies, organized by University of Oil and Gases, Faculty of Oil refining and Petrochemical, during the period 21-23 march 2012, Sinaia, Romania.

4. Cornelia – Magda Puscasu, **Mihaela Birsanu**, Carmen Gherasim, Gabriela Carja, Studies on the textural features of some layered double hydroxide matrices, at the conference The 7th International Conference on Advanced Materials ROCAM 2012, organized by the International Organization for Crystal Growth, by period 28 – 31 august 2012, Brasov, Romania.

5. Laura Dartu, **Mihaela Birsanu**, Magda Puscasu, Gabriela Carja, Studies on the nanoarchitectonic features of CuO-LDHs self-assemblies, at the conference „COST MPO904 Action „Single –and multiphase ferroics and multiferroics with restricted geometrie ”& the

9th Edition IEEE-ROMSC 2012”, organized by „Al. I. Cuza” University, during the period 24-26 September 2012, Iasi, Romania.

6. Magda Puscasu, **Mihaela Birsanu**, Carmen Gherasim, Gabriela Carja, Hydrotalcite – like anionic clays and their derived mixed oxides as highly efficient adsorbents for removing two industrial dyes from aqueous solutions, at the conference „International Conference ECOIMPULS 2012 – Environmental Research and Technology”, organizată de „Aquademica Romanian - German Foundation, Aquatim SA – the region’s water and wastewater operator, „Politehnica” University Timisoara, „Gheorghe Asachi,, Technical University of Iasi, during the period 25-26 october, Regional Business Center Timisoara, Romania.

7. Cornelia Magda Puscasu, **Mihaela Birsanu**, Carmen Gherasim, Gabriela Carja, Layered double hydroxides as catalysts in water splitting process, at the conference „International Conference Centenary of Education in Chemical Engineering”, organized by Technical University „Gheorghe Asachi”, Faculty of Chemical Engineering and Environmental protection, during the period 28-30 november 2012, Iasi, Romania.

Other activities

An external research internship during the period of 5 months at the Chemical Technology Institute, of the Polytechnic University of Valencia, Spain.

II. SELECTED RESULTS OF THE EXPERIMENTAL RESEARCH ACTIVITY; ORIGINAL CONTRIBUTIONS

II.1. SYNTHESIS AND PHYSICO-CHEMICAL CHARACTERIZATION OF LAYERED DOUBLE HYDROXIDES (LDHS) AND THEIR ME/LDHS NANOSTRUCTURED ASSEMBLIES (Chapter II and III in the Romanian version of the thesis)

LDHs based nanostructures have been obtained by using the structural reconstruction process of the LDHs in the aqueous solutions, type Me^+X^- . This has been afforded us to further manipulate the fabrication procedures of Me/LDHs and/or $\text{Me}_x\text{O}_y/\text{LDHs}$ nanostructures based on the LDHs reconstruction process.

This structural reconstruction is based on a very specific and interesting property of the LDHs, so-called structural ‘memory effect’. This means that the layered clay structure, that can be destroyed by calcination at moderate temperatures (ca. 550°C) to yield low crystalline mixed oxides, can be reconstructed in aqueous solutions containing anionic species. Up to this moment it is clear for us that during the LDHs reconstruction the anions of the solutions will be taken to serve as interlayer anions of the LDHs matrix though we have limited knowledge of how the cations of the solutions are organized in the form of nanoparticles on the surface of the large nanoparticles of the LDHs. In this reason the research activity was focused to deeply study of the LDHs reconstruction process in the aqueous solutions of gold salts ($\text{Au}^{y+}\text{X}^{3-}$) and the aqueous solutions of iron salts ($\text{Fe}^{y+}\text{X}^{3-}$). Not only the different Me^+X^- solutions but also the tailored composition of the LDHs was one of controlled variable (e.g. MgAlLDH, ZnAlLDH, FeLDH, ZnCeAlLDH).

II.1.1. Fabrication of layered double hydroxides LDHs and their Me/LDHs nanostructured assemblies

Layered double hydroxides LDHs were synthesized by direct co-precipitation methods at constant pH, figure II.1 illustrating the final experimental protocol.

Synthesis of layered double hydroxides LDHs

ZnAlLDH: 500 ml of the aqueous solutions of the metal salts used as precursors ($\text{Zn}(\text{NO}_3)_2 \cdot 6\text{H}_2\text{O}/\text{Al}(\text{NO}_3)_3 \cdot 9\text{H}_2\text{O}$) with the Zn/Al molar ratio 2:1 and aqueous solutions (1 M) of the precipitants $\text{NaOH}/\text{Na}_2\text{CO}_3$ were added together at 37°C and a constant pH ~ 9.

ZnCeAlLDH: 500 ml of the aqueous solutions of the metal salts used as precursors ($\text{Zn}(\text{NO}_3)_2 \cdot 6\text{H}_2\text{O}$ / $\text{Ce}(\text{NO}_3)_3 \cdot 6\text{H}_2\text{O}$ / $\text{Al}(\text{NO}_3)_3 \cdot 9\text{H}_2\text{O}$) with the Zn:Ce:Al molar ratio 2:0.3:0.7 and aqueous solutions (1 M) of the precipitants NaOH/ Na_2CO_3 were added together at 37°C and a constant pH ~ 9.

The obtained precipitates were aged at 45°C for 20 h, separated by centrifugation, washed extensively with warm double deionized water until they were sodium free and dried in the oven at 90°C. After calcination at 750°C for 8 h, these samples were denoted as ZnAlLDH750 and ZnCeAlLDH750, respectively.

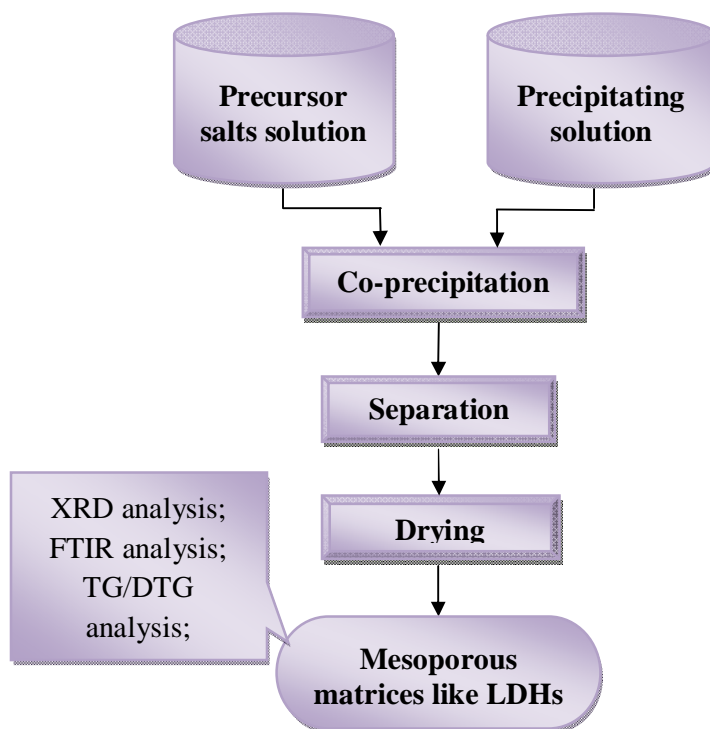


Figure II.1. Experimental protocols for obtaining layered double hydroxides LDHs using the co-precipitation method and the main characterization techniques

ZnCeAlLDH2: 500 ml of the aqueous solutions of the metal salts used as precursors ($\text{Zn}(\text{NO}_3)_2 \cdot 6\text{H}_2\text{O}$ / $\text{Ce}(\text{NO}_3)_3 \cdot 6\text{H}_2\text{O}$ / $\text{Al}(\text{NO}_3)_3 \cdot 9\text{H}_2\text{O}$) with the Zn:Ce:Al molar ratio 2:0.4:0.8 and aqueous solutions (1 M) of the precipitants NaOH/ Na_2CO_3 were added together at 37°C and a constant pH ~ 9.

The obtained precipitates were aged at 45°C for 20 h, separated by centrifugation, washed extensively with warm double deionized water until they were sodium free and dried in the oven at 90°C. After calcination at 750°C for 8 h, these samples were denoted as ZnAlLDH750 and ZnCeAlLDH750, respectively.

MgAlLDH: 250 ml of an aqueous solution of $\text{Mg}(\text{NO}_3)_2 \cdot 6\text{H}_2\text{O}$ (0.1 mol)/ $\text{Al}(\text{NO}_3)_3 \cdot 9\text{H}_2\text{O}$ (0.05 mol) and an aqueous solution of NaOH/ Na_2CO_3 were added dropwise together in such a

way that the pH remained at a constant value of 10. The obtained precipitates were aged at 65°C for 12 h, separated by centrifugation, washed extensively with warm deionized water until sodium free and dried in the oven at 90°C.

MgFeAILDH: Iron containing hydrotalcite – like anionic clay was synthesized by the co-precipitation method following the procedure by Reichle; 250 mL of the aqueous solutions of the metal salts used as precursors ($\text{Mg}(\text{NO}_3)_2 \cdot 6\text{H}_2\text{O}:\text{Fe}(\text{NO}_3)_3 \cdot 9\text{H}_2\text{O}:\text{Al}(\text{NO}_3)_3 \cdot 9\text{H}_2\text{O}$ – molar ratio 2:0.7:0.3) and the aqueous solution (1M) of the precipitants $\text{NaOH}/\text{Na}_2\text{CO}_3$ were added drop wise together at 45°C, at the constant pH of 10.

The orange precipitate was aged 65°C for 1h, separated by centrifugation, washed extensively with double deionized water until sodium free and dried in oven overnight and was denoted as FeLDH.

Synthesis of Me/LDHs and Me_xO_y/LDHs nanostructured assemblies

The precursor anionic clays ZnAILDH, ZnCeAILDH and MgFeAILDH obtained by the co-precipitation method were calcined at 550°C for 14h with a heating rate of 8° C·min⁻¹. The samples were obtained following the experimental procedure:

Au/LDHs: 1g of the freshly calcined clay was added, under magnetic stirring in 0.1M aqueous solution of AuCl_3 (Sigma Aldrich), the reconstructed medium having the pH value approximately equal to 9. The obtained samples were aged at the ambient temperature for 45 min, centrifuged, washed with distilled water, dried under vacuum and denoted as Au/ZnAILDH and Au/ZnCeAILDH. These samples were calcined at 750° for 8h and denoted as Au/ZnAILDH750 and Au/ZnCeAILDH750.

Au/ZnCeAILDH2: Au/ZnCeAILDH2: 1g of “freshly” calcined clays (in this case calcinations was done at 550°C for 9 h) was added, under vigorous stirring in 150 mL of a 0.1 M aqueous solution of AuCl_3 . Cl^- was used as an anion source for the structural reconstruction of the clay interlayer. The obtained sample were aged at room temperature for 1h, washed with double deionized water, dried in air and were denoted as Au/ZnCeAILDH2 .

After calcinations at 600°C for 8h the samples Au/ZnCeAILDH and Au/ZnCeAILDH2 were denoted as Au/ZnCeAILDH1 600 and Au/ZnCeAILDH2 600, respectively.

Fe₂O₃/FeLDH that as denoted Fe/FeLDH: 1g of freshly calcined FeLDH powder was added to an aqueous solution (0.5M) of FeSO_4 at a constant pH, approximately 9, under magnetic stirring. The volume of the aqueous solutions of the metal salts was calculated such that the SO_4^{2-} concentration has exceeded the exchange capacity of the clay (Carja et al., 2008). The obtained precipitates were aged at 65°C and denoted Fe/FeLDH1 and Fe/FeLDH2, the differences consisting at the time that the clay was kept in the aqueous salt solution (12.5 min, respectively 25 min).

The synthesized protocol is described schematically in figure III.1.

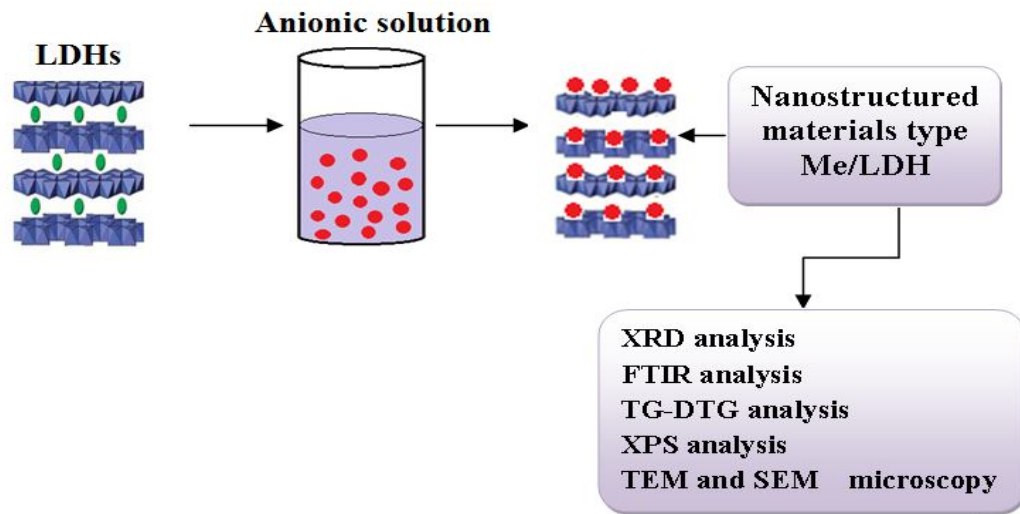


Figure III.1. Experimental protocols for obtaining nanostructured material type Me/LDHs

II.1.2. Au/LDHs as nanostructured assemblies; studies of physical-chemical properties

Structural characteristics of Au/LDHs described by X-ray diffraction (XRD) and X-ray photoelectron spectroscopy (XPS)

XRD analysis is a physico-chemical technique which provides information about the chemical composition and crystallographic structure of hydrotalcite like anionic clays LDHs.

The structural characteristics of Au/LDHs nanostructured materials were recorded by X-ray diffraction (XRD), figure III.2A showing the XRD patterns of Au/ZnAlLDH. This reveals the presence of a single crystalline phase with reflections assigned to the regular layered structure of hydrotalcite like anionic clay, defined by a series of sharp and symmetric basal reflections of the 003, 006 and 009 planes and broad, less intense reflections for the nonbasal 012, 015 and 018 planes.

No peak characteristic of the gold phase can be noticed, because it is possible that the small and highly dispersed Au nanoparticles could not be detected by XRD. Further information about the structural characteristics have been identified by XRD analysis of the calcined samples at 750°C, because the calcinations process has a major influence on the structural features of the hydrotalcite-like anionic clay.

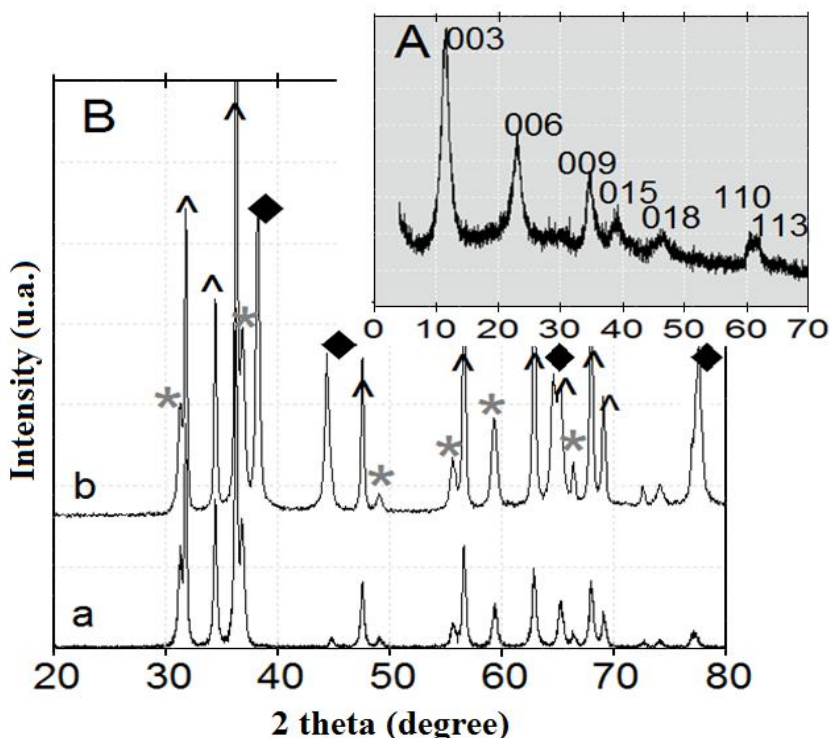


Figure III. 2. (A) XRD patterns of Au/ZnAlLDH (B) XRD patterns of a) ZnAlLDH750 and b) Au/ZnAlLDH750; (♦) Au; (*) ZnAl₂O₄; (Δ) ZnO.

Figure III.2B presents the comparison of the XRD pattern of ZnAlLDH750 and Au/ZnAlLDH750. The characteristic reflections of ZnO and ZnAl₂O₄ can easily be observed in each case.

However, the XRD pattern of Au/ZnAlLDH750 shows four new well developed reflections at $2\theta = 38.1, 44.3, 64.5$ and 77.4° , assigned to the diffraction lines of the (111), (200), (220) and (311) planes of the face-centered cubic (FCC) of gold clearly confirming the presence of crystalline Au in Au/ZnAlLDH750.

Figure III.3 presents the XRD patterns of ZnCeAlLDH750 and Au/ZnCeAlLDH750. For ZnCeAlLDH750, we have observed some sets of diffraction peaks; they can be indexed to the hexagonal wurtzite ZnO, ZnAl₂O₄ spinel and the face-centered cubic (FCC) structure of CeO₂. This is in agreement with previously published results that demonstrate the presence of crystalline CeO₂ as a component of the mixtures of mixed oxides formed after the calcination of LDHs containing cerium in the layers. In comparison, the XRD pattern of Au/ZnCeAlLDH750 clearly shows additional reflections at $2\theta = 38.1, 44.3, 64.5$ and 77.4° , assigned to the diffraction lines of the (111), (200), (220) and (311) planes of the face-centered cubic (FCC) of gold crystallites, thus further confirming the presence of crystalline gold in Au/ZnCeAlLDH750.

The above data point to the fact that after calcination at 750°C, the anionic clay supports gave rise to complex composition types ZnO/ZnAl₂O₄ and CeO₂/ZnO/ ZnAl₂O₄, on which larger Au NPs are well dispersed.

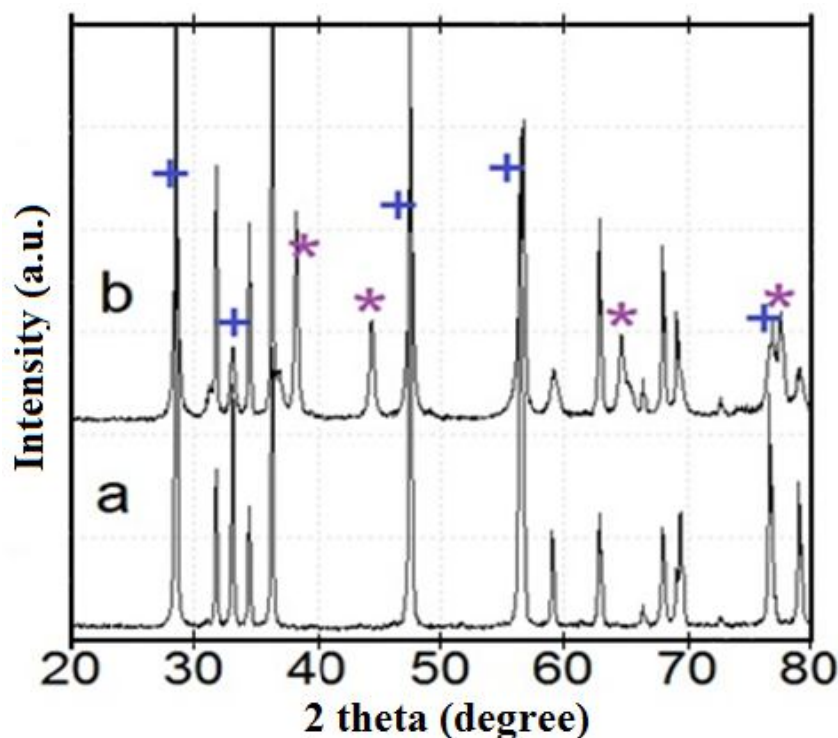


Figure III.3. XRD patterns of (a) ZnCeAlLDH750 and (b) Au/ZnCeAlLDH750; (+) CeO₂; (*) Au.

Table 1 summarizes the average sizes (D_{Au}) and the external surface area (S_{Au}) of the AuNPs, calculated according to the procedure reported by Tanaka et al. for Au NPs loaded on cerium oxide (Au/CeO₂).

The S_{Au} values of Au/ZnAlLDH and Au/ZnCeAlLDH are 3.97m²g⁻¹ and 3.43m²g⁻¹, respectively. The S_{Au} values decrease almost ten times after calcination and the S_{Au}/S_{BET} ratio decreases from 0.06 for Au/LDHs to 0.01 after calcination at 750°C. Furthermore, the contribution of the mesopore area in the total t-plot area is around 80% for all the LDHs revealing the mesoporous characteristics of LDH clays.

The chemical states of the Au species on the catalyst surface were studied by X-ray photoelectron spectroscopy (XPS). The results show that Au/ZnAlLDH consists mainly of 53.7 atom% of oxygen, 14.7 atom% of zinc, 3.5 atom% of aluminum and 3.7 atom% of gold while Au/ZnCeAlLDH consists of 54.1 atom% of oxygen, 14.1 atom% of zinc, 2.5 atom% of cerium, 2.2 atom% of aluminum and 3.9 atom% of gold, as can be seen in table III.2.

Table 1. Various physical-chemical properties of the catalysts.

Catalyst	D_{Au} (nm)	$S_{Au} \cdot 10^{-2}$ (m^2/g)	S_{BET} (m^2/g)	$S_{Au} \cdot 10^{-2}/S_{BET}$	XPS	ICP
					Au atomic ratio (%)	
ZnAlLDH	-	-	83 (87) ^a	-	-	-
Au/ZnAlLDH	2.9	3.9	55 (79) ^a	0.067	3.7	3.9
Au/ZnAlLDH 750	37	0.35	334	0.01	4.1	4.0
ZnCeAlLDH	-	-	77 (89) ^a	-	-	-
Au/ZnCeAlLDH	3.4	3.43	51 (83) ^a	0.065	3.9	4.0
Au/ZnCeAlLDH 750	40	0.34	29	0.01	4.1	4.0

$S_A = 3W_A/\rho D_{Au} / 2.$
 ρ - Au density 19.32 g/cm³
 ()^a : % mesopore area in the t-plot area.

The high resolution XPS spectrum of the Au 4f region presented similar features for both Au/ZnAlLDH and Au/ZnCeAlLDH. Figure III.4 shows the Au 4f region of the XPS spectra of Au/ZnAlLDH.

Table III.2. Au/LDHs nanostructured materials composition according with X-ray photoelectron spectroscopy

Sample	Zn (%)	Au (%)	Al (%)	O (%)	Ce (%)
Au/ZnAlLDH	14.7	3.7	3.5	53.7	-
Au/ZnCeAlLDH	14.1	3.9	2.2	54.1	2.5

The relative intensity of the peaks corresponding to each oxidation state reveal that for Au/ZnAlLDH, 87% of the Au of the surface existed in the metallic state while the contribution of metallic gold reaches 83% for Au/ZnCeAlLDH.

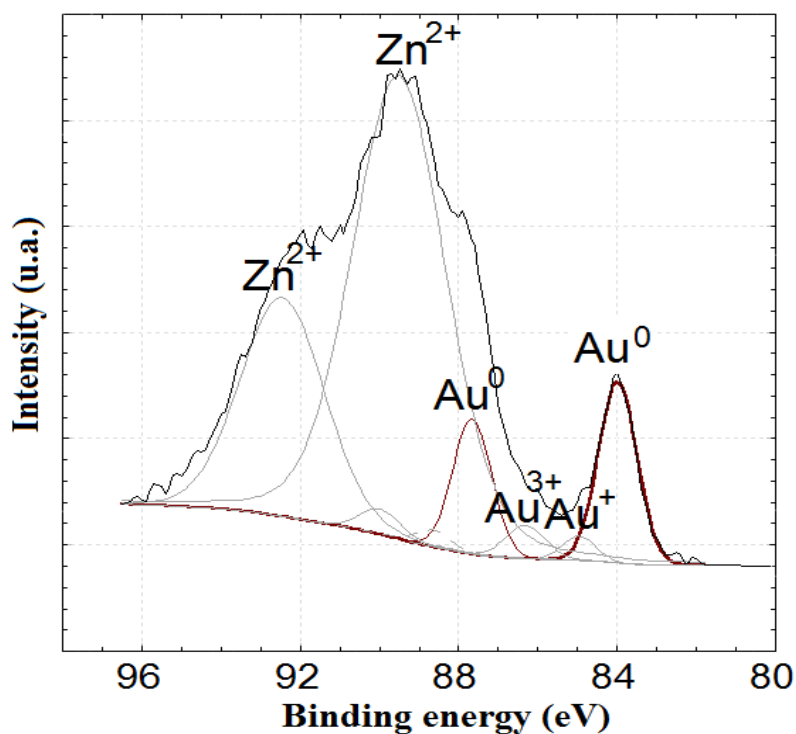


Figure III.4. High resolution XPS spectra of Au 4f for Au/ZnAlLDH.

The presence of gold mainly in the metallic state on the surface of LDHs is attributed to the instability of cationic gold that can be reduced at room temperature even under an oxygen atmosphere; these observations are consistent with the results reported for Au/ZnO composites.

Nature of layered double hydroxides interlayer anions studied by Fourier transforms infrared spectroscopy (FTIR)

To determinate the structural characteristics of the studied samples has been used FTIR technique, which provide information about the anions nature from the brucite like layers, figure III.6 illustrating the FTIR spectra of the precursor layered double hydroxides LDHs compared with nanostructured materials type Au/LDHs. For all samples, the strong band around 3460 cm^{-1} is associated with the stretching vibration of OH groups in the brucite like layers and the interlayer water molecules.

The broadening of the band was attributed to the hydrogen-bond formation. Less intense absorption bands around $1620\text{-}1500\text{ cm}^{-1}$ was assigned to the bending vibration of interlayer water molecules.

If the corresponding FTIR spectra of the LDHs precursors shows the presence of a strong absorption band at 1360 cm^{-1} associated with the vibration mode ν_3 of carbonate anions, in case of reconstructed clays, this band is slightly shifted up to the wavenumber equal to 1380 cm^{-1} due to the chloride anion presented in the gold chloride aqueous solutions, following the reconstruction clays and the specific interactions of the parent clays with the anion solution. For the clays containing cerium ions in the structure can be observed that the characteristic peak of the CO_3^{2-} anion is less intense than in case of ZnAILDH and Au/ZnAILDH clays.

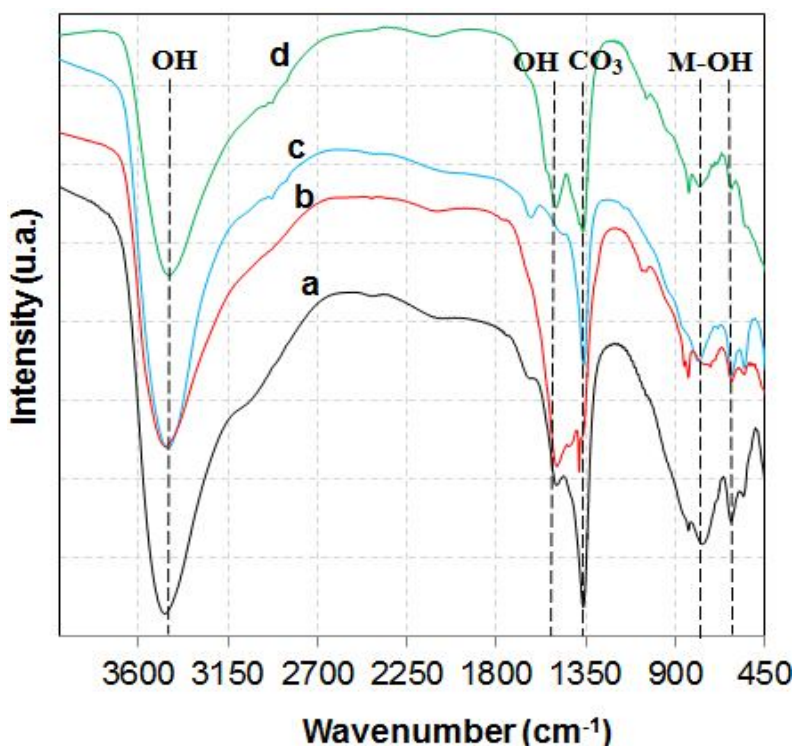


Figure III.5. FTIR spectra for a) ZnAILDH; b) ZnCeAILDH; c) Au/ZnAILDH; d) Au/ZnCeAILDH

For all the samples in the low wavenumber region ($< 1000\text{ cm}^{-1}$), the lattice vibration modes of the LDHs sheets such as M-O between $840\text{-}550\text{ cm}^{-1}$ and M-O-M ($< 500\text{ cm}^{-1}$) vibration are observed.

Nanostructured assembly type Au/LDHs were also characterized in terms of thermal behavior. Information about temperatures ranges for each phase of the thermal degradation process are shown in table III.3. From table III.3 can be seen that although the steps of thermal degradation are approximately similar, the mass loss of reconstructed clays in aqueous solution of AuCl_3 based on structural memory effect is less and equal to 30% for Au/ZnAILDH and only 19% for Au/ZnCeAILDH clays.

Table III.3. Numerical data about the thermal degradation process of layered double hydroxides (LDHs)

Sample	Stage	Temperature (°C)			Mass loss (%)	
		T _i (°C)	T _m (°C)	T _f (°C)	Each step (%)	Totally (%)
ZnAlLDH	I	31.2	193.21	215.6	15.8	34.28
	II	216.6	259.8	437.38	18.48	
Au/ZnAlLDH	I	31.42	134.93	147.73	5.501	30.69
	II	147.73	197.82	233.45	10.22	
	III	233.45	359.32	501.94	10.519	
	IV	501.94	596.34	900	4.455	
ZnCeAlLDH	I	30.35	76.73	133.49	4.34	27.21
	II	133.49	173.84	206.26	5.41	
	III	206.26	282.47	600	17.46	
Au/ZnCeAlLDH	I	31.42	84.89	128.23	1.724	18.85
	II	128.23	185.85	216.5	4.646	
	III	216.5	266.55	664.27	12.486	

T_i – initial temperature of thermal degradation;
T_m – medium temperature of degradation;
T_f – final temperature of thermal degradation process

The results show that the thermal stability is influenced by the chemical composition and the structure of the reconstructed clays. From the comparative analysis regarding the thermal degradation of these two nanostructured materials can be observed that the derived material type Au/ZnAlLDH has a higher thermal stability compared to the Au/ZnCeAlLDH clay.

Micromorphology and textural characteristics of Au/LDHs describes by field emission electron microscopy (FESEM) and transmission electron microscopy (TEM)

To identify the textural characteristics of the derived materials Au/LDHs were used modern analytical techniques, important information providing by scanning electron microscopy (SEM) and transmission electron microscopy (TEM). SEM images of LDHs and Au/LDHs nanostructured materials are shown in figure III.9.

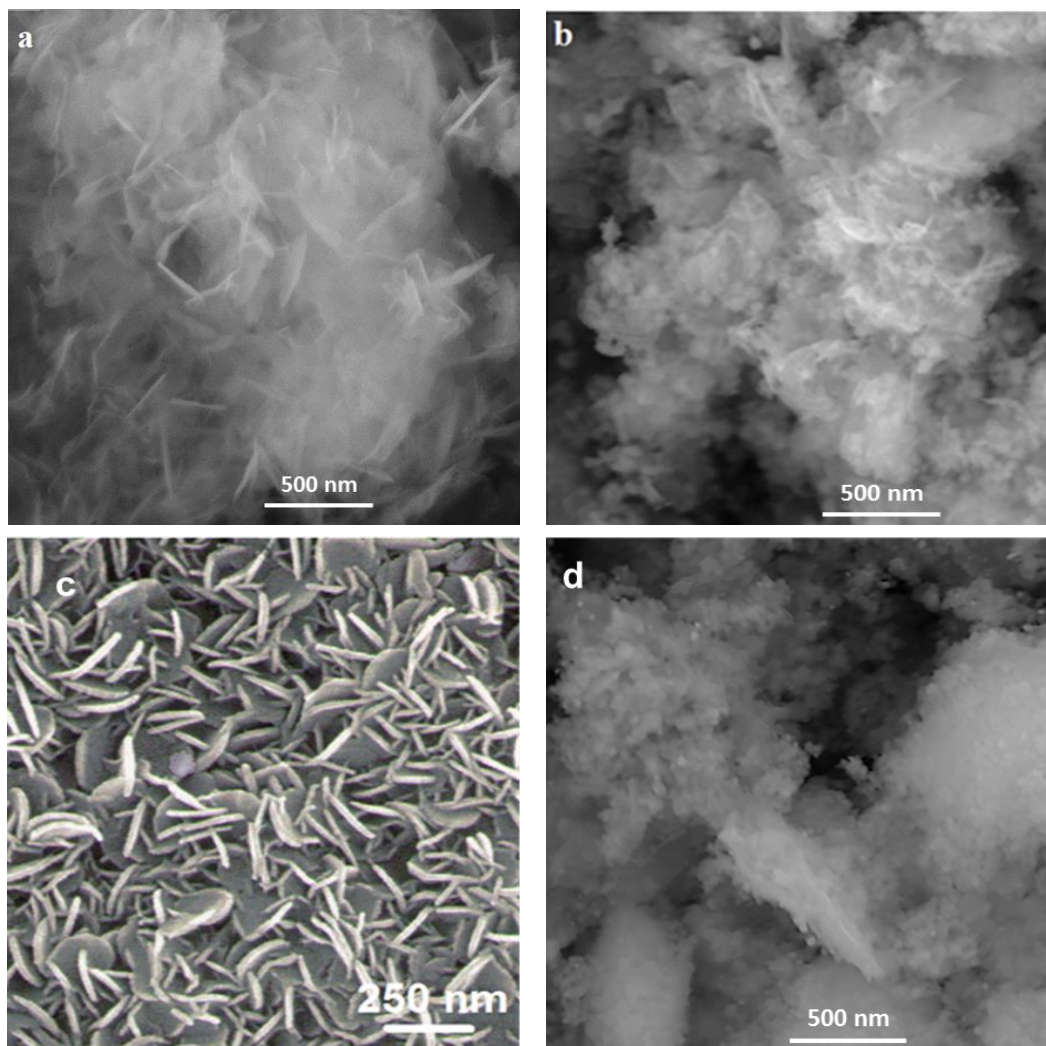


Figure III. 9. SEM images of a) ZnAILDH; b) ZnCeAILDH; c) Au/ZnAILDH; d) Au/ZnCeAILDH at different magnification

The figure above illustrates that layered double hydroxides LDHs presents morphological characteristics of hydrotalcite compounds, with platelet like particles, closed connected one to another, giving rise to a particular textural arrangement, known in the literature as “sand-rose” packing and that Au/LDHs exhibits also the conventional LDH morphology consisting of aggregates of platelet-like particles with average sizes of 110 nm. These results are consistent with the literature dates (Ballarin et al., 2012).

In the typical TEM image of Au/ZnAILDH (see Fig. III.10a), very small Au NPs can be clearly observed as dark spots highly dispersed on the larger particle of the clay; the average size of the loaded Au NPs is 2.9 nm. The HRTEM image, as presented in Fig. III.10c, indicates that the small Au NPs are highly crystalline with a well-defined spacing of ca. 0.24 NM between adjacent lattice fringes, close to the d- spacing value of the (111) plane of FCC gold.

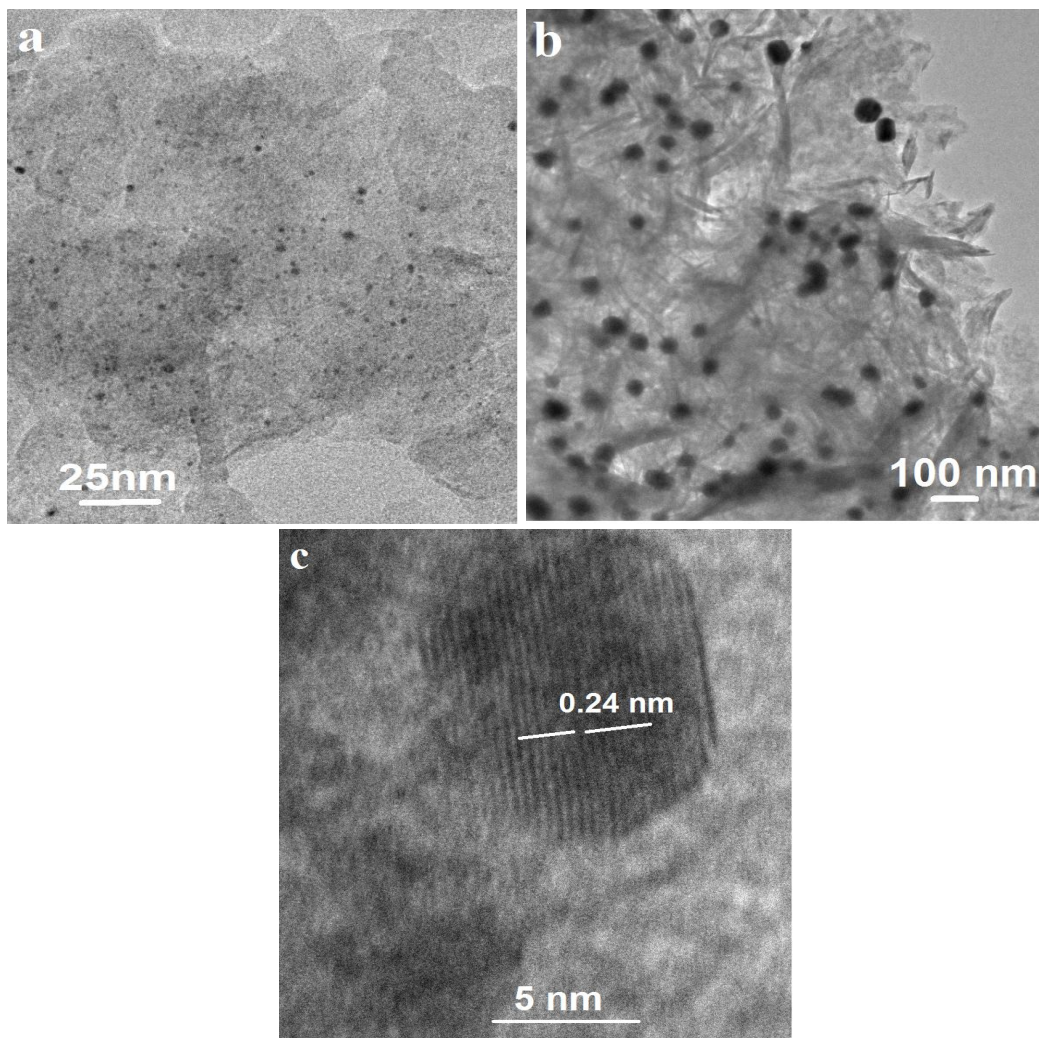


Figure III.10. TEM images for: a) Au/ZnAILDH; b) Au/ZnAILDH750; c) HRTEM image of Au/ZnAILDH.

Figure III.10b shows a typical TEM image of Au/ZnAILDH750. It is important to note that after calcination at 750°C, the average size of the loaded Au NPs increases up to 37 nm while, importantly, they are still highly dispersed on the anionic clay. Previous results attributed such a significant size increase (more than 10-fold) of Au NPs deposited on a porous matrix to the fusion process of NPs during the thermal treatment. Moreover, the large size increase of Au NPs shows the absence of a strong metal–support interaction effect (SMSI) between the loaded NPs and the clay support.

A typical TEM image of Au/ZnCeAILDH (Figure III.11A) shows that the NPs with an average size of 3.4 nm are highly dispersed on the clay. After calcination at 750°C, the average diameter of the loaded NPs reaches almost 40 nm (see Figure III.11B).

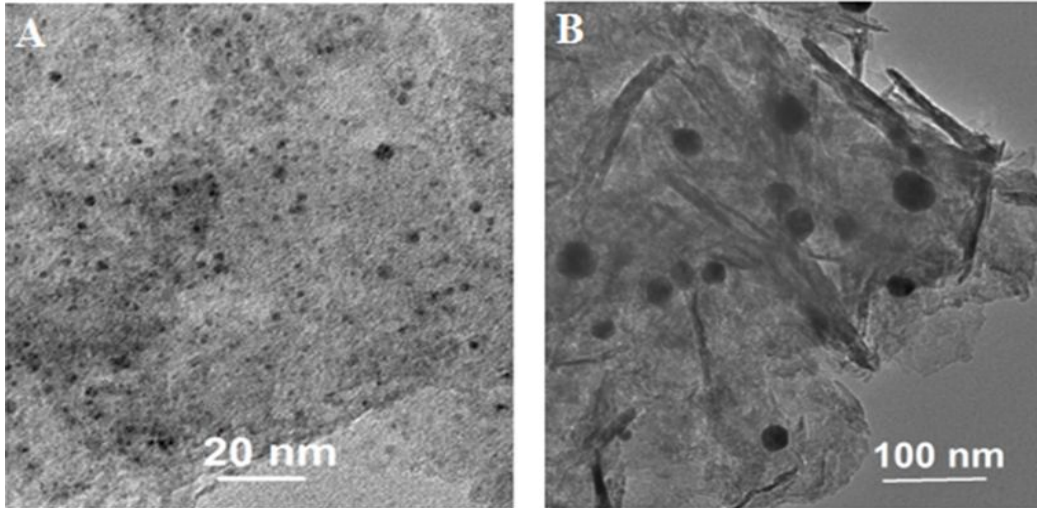
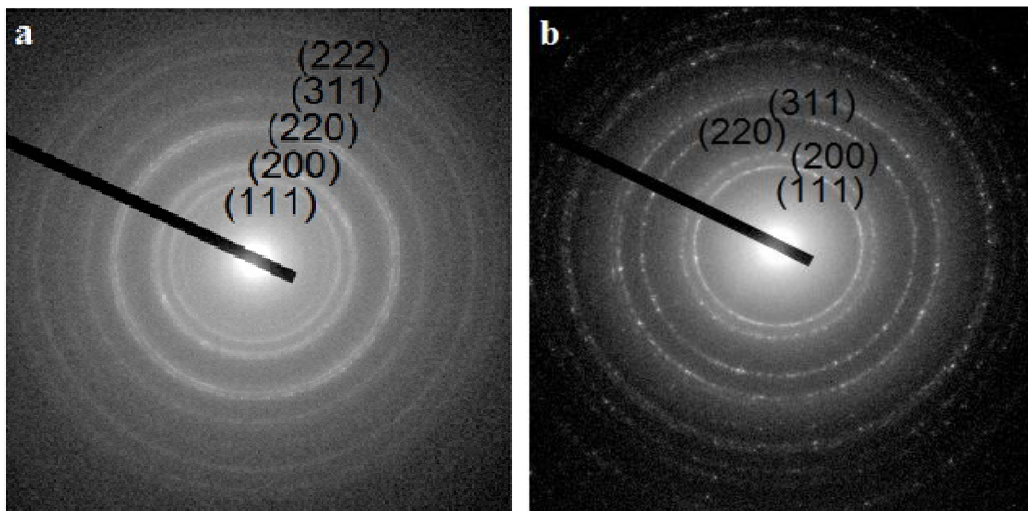


Figure III.11. TEM micrographs for (A) Au/ZnCeAILDH; (B) Au/ZnCeAILDH750

The SAED patterns for the samples Au/ZnAILDH and Au/ZnAILDH750, shown in figure III.12a and b, present a set of diffuse diffraction rings in which the (111), (200), (220), (311) and (222) reflections of FCC gold can be indexed.



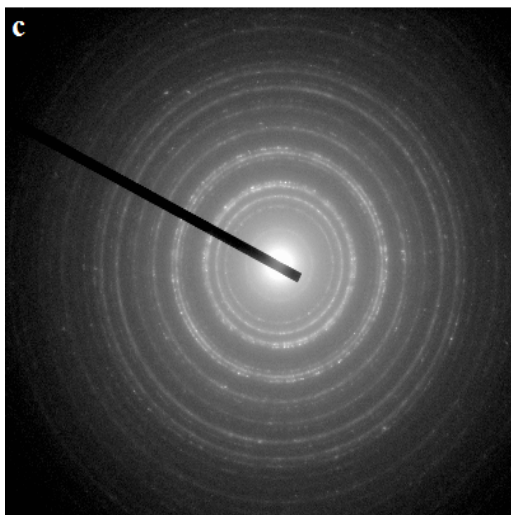


Figure III.12. SAED patterns for nanostructured materials type a) Au/ZnAILDH; b) Au/ZnAILDH750; c) Au/ZnCeAILDH750.

The SAED pattern of Au/ZnCeAILDH750 (shown in figure III.12 c) reveals some sets of zone diffraction patterns, thus indicating complex structural features, obtained after the calcination process.

The textural characteristics have been analyzed after the calcination process at 750°C for the reconstructed clays Au/LDHs750 in order to observe the modification that occur at the structural level (figure III.13).

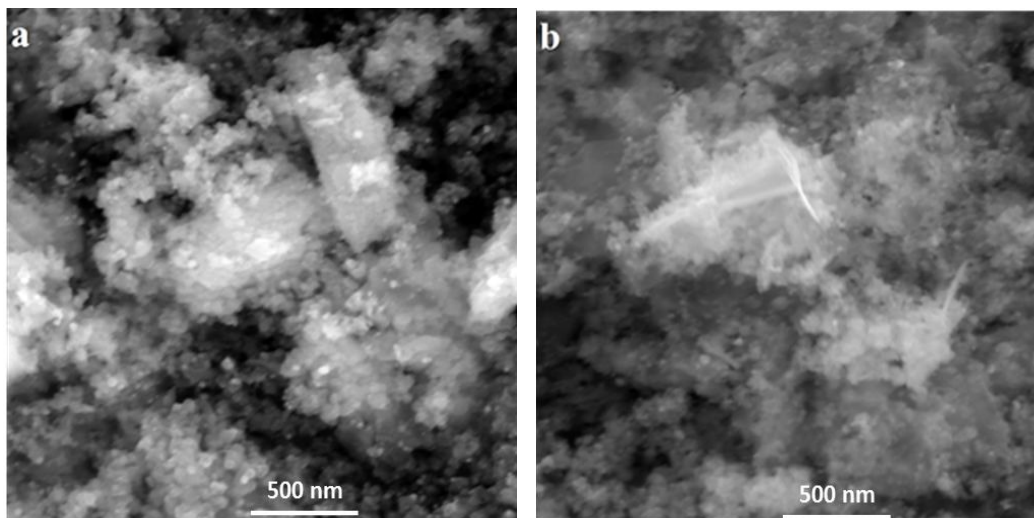


Figure.III.13. SEM images for a) Au/ZnAILDH750; b) Au/ZnCeAILDH750.

After calcination process, SEM images exposed that the lamellar structure collapse, with the formation of a new different crystallites type derived mixed oxides derives also with Au nanoparticles uniformly distributed on the surface of anionic clays used as support.

The XRD, XPS and TEM results strongly support the formation of specific nanoarchitectures described as plasmonic gold nanoparticles loaded onto the larger nanoparticles of ZnAlLDH and ZnCeAlLDH mesoporous clays. Under calcination at 750 °C, the anionic clay supports undergo phase transformations into ZnO/ZnAl₂O₄ and CeO₂/ZnO/ZnAl₂O₄ solutions while the loaded plasmonic Au nanoparticles increase their size though they are still highly dispersed on the clay supports.

II.1.3. Fe/FeLDH as nanostructured assemblies; studies of physical-chemical properties

Structural characterization of Fe/Fe/LDH by XRD and FTIR analyses

The XRD patterns of the field as synthesized and reconstructed samples shows the double layered hydroxides structure in all samples (figure III.14), with sharp and symmetric basal reflections of (003), (006) and (009) planes, at a low 2θ angle and broad, less intense and asymmetric reflection of the non-basal (012), (015) and (018) plane, at a high 2θ angle.

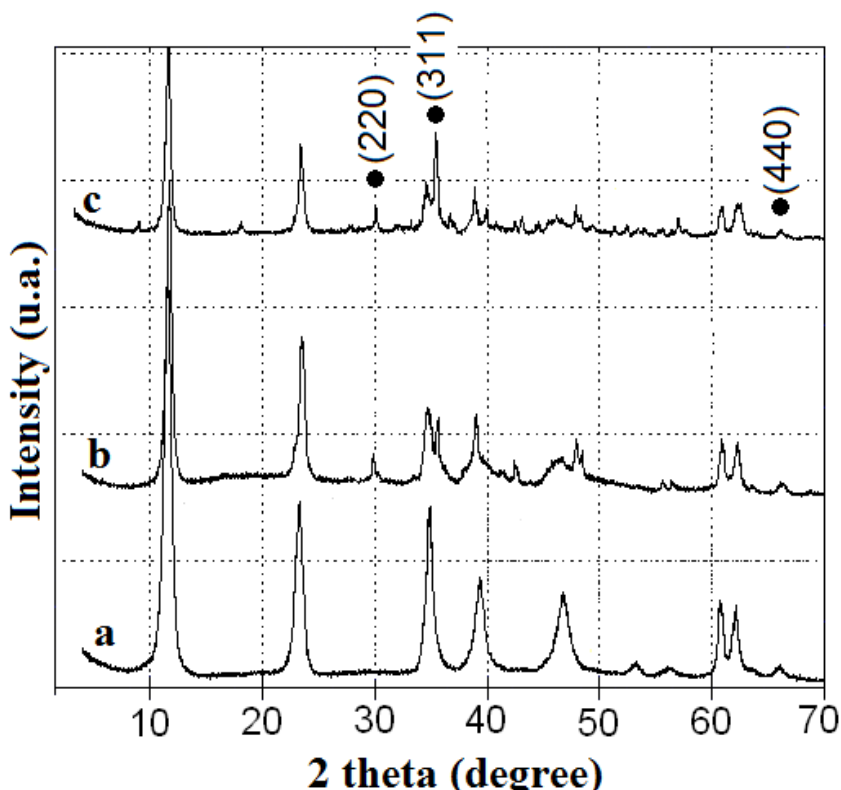


Figure III.14. The XRD pattern of: a) FeLDH; b) Fe/FeLDH1; c) Fe/FeLDH2

(●) Fe₃O₄ or γ-Fe₂O₃

For Fe/FeLDH1 and Fe/FeLDH2 the intensity of the diffraction peaks decreases in comparison to the original iron substituted clay; this may be a consequence of a lower crystallinity or different textural characteristics of the materials (Carja et al., 2005).

The XRD patterns of the reconstructed clays clearly show new diffraction peaks that match well with the characteristic reflections of Fe₃O₄ or γ -Fe₂O₃; however it is well known that clear identification of Fe₃O₄ and γ -Fe₂O₃ (based on XRD analysis) are difficult due to their similar XRD pattern and lattice parameters. XRD analysis reveals that we obtained iron oxide Fe₂O₃ supported on iron substituted clay. The XRD reflections were indexed assuming a hexagonal cell with the rhombohedral lattice (R – 3m). The cell parameter *a* is a function of the metal – metal distance within the layers and the *c* parameter is associated with the layer to layer distance.

The parameter *a* is equal to 3.047 nm for the as synthesized clay FeLDH and its value increase to 3.049 and 3.057 nm for Fe/FeLDH1 and Fe/FeLDH2. For the *c* parameter, its value increase from 23.39 nm for FeLDH to 23.79 and 24.07 nm for the reconstructed clays Fe/FeLDH1 and Fe/FeLDH2.

The modified value of these parameters can be explained by the elongation of the metal – oxygen bond distance, but also by the new specific electrostatic features of the synthesis medium when is used as anion source an aqueous solution of SO₄²⁻. This increase was also reported by Refait et al. (2005) when the SO₄²⁻ replaced the anions on the synthesis medium of iron containing LDH.

The result of the quantitative analysis, carried out by ICP emission spectroscopy and XRD structural parameters of the materials are presented in Table 1. The decrease of the surface area and the pore volume for the reconstructed clays can suppose less emphasized porous property for the iron oxide hydrotalcite.

Table III.4. Chemical composition, lattice parameters and some textural parameters of the anionic clay – like studied samples

Sample	Fe (% mass)	Lattice parameters (nm)		S _{BET} (m ² /g)	V _p (cm ³ /g)
		<i>a</i>	<i>c</i>		
FeLDH	28.4	3.047	23.39	127	0.377
Fe/FeLDH1	35.7	3.049	23.79	91	0.272
Fe/FeLDH2	41.5	3.057	24.07	67	0.254

For structural characterization of studied anionic clays has been used Fourier transform infrared spectroscopy in order to identify the anionic species from the interlayer region and also to determine the substitution of Fe³⁺ ions in the brucite like layers. Figure

III.15 present the comparison of the FTIR spectra for layered double hydroxides LDHs precursors and the reconstructed clays.

Analyzing the FTIR spectra it can be observed an absorption band located at 3450 cm^{-1} attributed to the stretching vibration of the hydroxyl group ($\nu_{\text{O-H}}$), from the clay layers, the absorbed water molecules and also the interlayer water.

A weak band can be seen at 3000 cm^{-1} due to the hydrogen bonds connecting water molecules and the anions from the interlayers region.

Another absorption band, similar to that of parent clay is situated at 1650 cm^{-1} associated with the deformation vibration of water molecules. The absorption peak in the wavenumber range $1380\text{-}1360\text{ cm}^{-1}$ is assigned to the asymmetric vibration mode of carbonate anions ν_3 or nitrate anions, if they are still present in the brucite like layers.

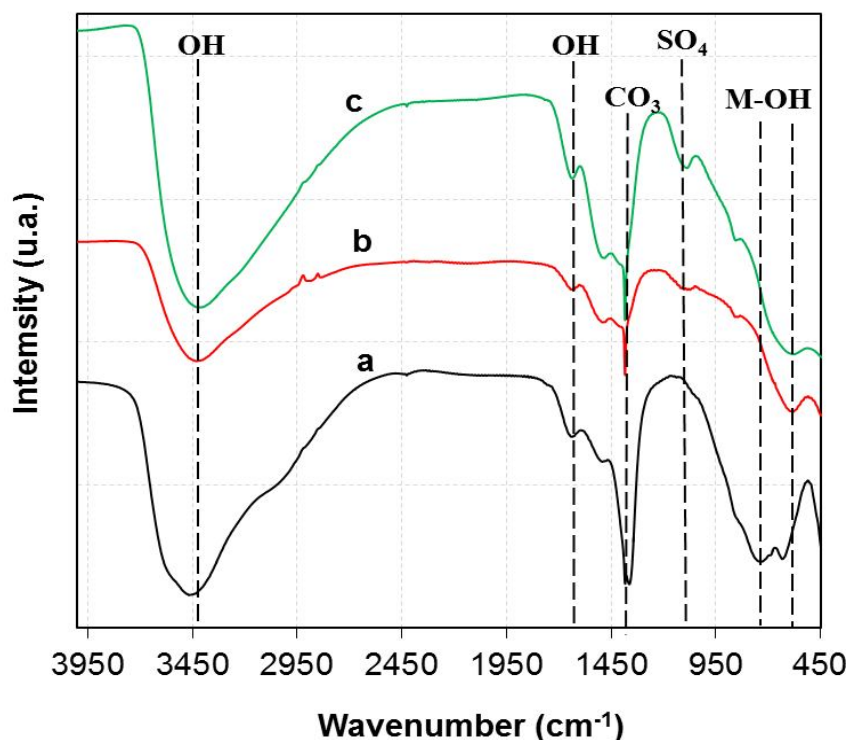


Figure III.15. FTIR spectra for a) FeLDH; b) Fe/FeLDH1; c) Fe/FeLDH2.

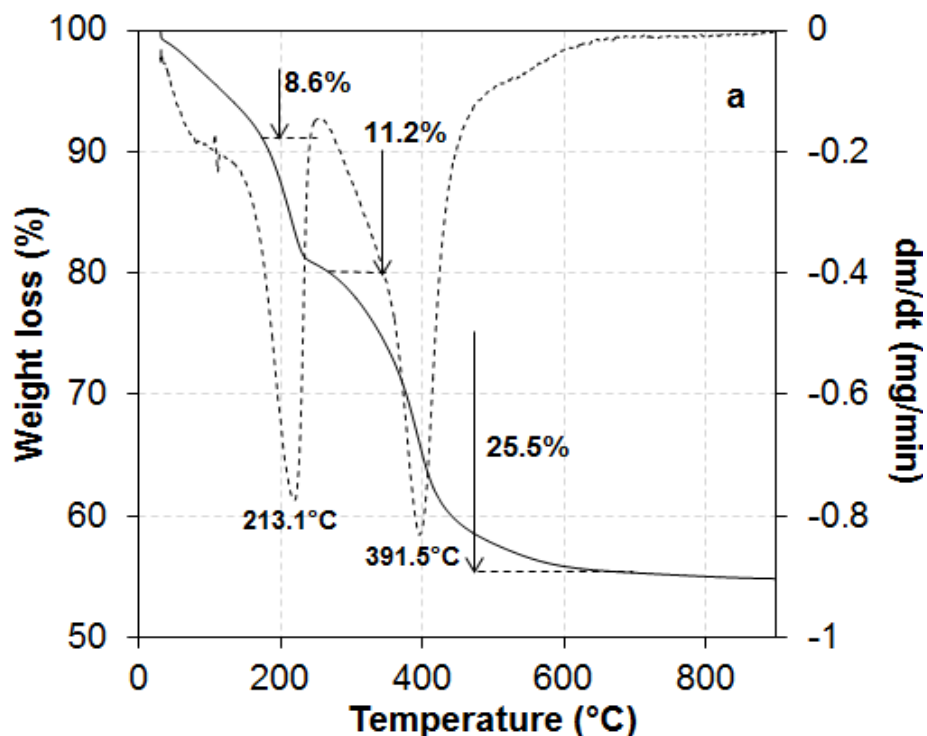
For the reconstructed clays $\text{Fe}_2\text{O}_3/\text{MgFeAlLDH}$ denoted Fe/FeLDH obtained after the reconstruction process in ferrous sulfate solution, FTIR spectra shows a new absorption band situated at 1080 cm^{-1} associated with the vibration mode of the ν_3 sulfate anions from interlayer region. Characteristics vibrations of carbonate anions can be observed after the reconstruction process, by less intense absorption bands; it can be explained that the removal of CO_3^{2-} anions from the interlayer space was not complete and in the interlayer region of Fe/FeLDH besides sulfate anions exist also carbonate anions.

In the low wavenumber region ($<1000\text{ cm}^{-1}$) the lattice vibration modes of the LDH sheets such as M–O (580 and 749 cm^{-1}) and O–M–O ($450 - 660\text{ cm}^{-1}$) vibrations are observed.

Nanostructured materials type Fe/FeLDH was studied in terms of thermal behavior using the TG-DTG technique. Thermal decomposition of iron oxide assemblies – layered double hydroxides is shown in figure III.16.

TG-DTG profiles allow the identification of temperature ranges and mass loss of Fe/FeLDH anionic clays. In the case of nanostructured materials Fe/FeLDH is noticed that the thermal degradation process takes place in three stages. In the first stage, in a temperature range of $29.19 - 124.72^\circ\text{C}$ occur the loss of absorbing water and the water molecules from the interlayer region. This peak is slightly shifted compared with the corresponding peak of the first stage of thermal degradation of the parent clay FeLDH. The mass loss in case of reconstructed clays is 5.13% , lower than the mass loss for the layered double hydroxides precursors (8.67%).

The second stage of $127.2 - 329.52^\circ\text{C}$ is attributed to the weight loss due to the decomposition of interlayer anions and also in the dehydroxylation process of the brucite like layers; the weight loss in this case was 10.81% . For the reconstructed clays in sulfate iron solution endothermic processes take place. The final stage of thermal degradation is attributed to the collapse of the layered structure for both parent and reconstructed clays, with the formation of mixed oxides. In this last stage the mass loss was about 4.451% . The overall weight loss for Fe/FeLDH was 20.38% .



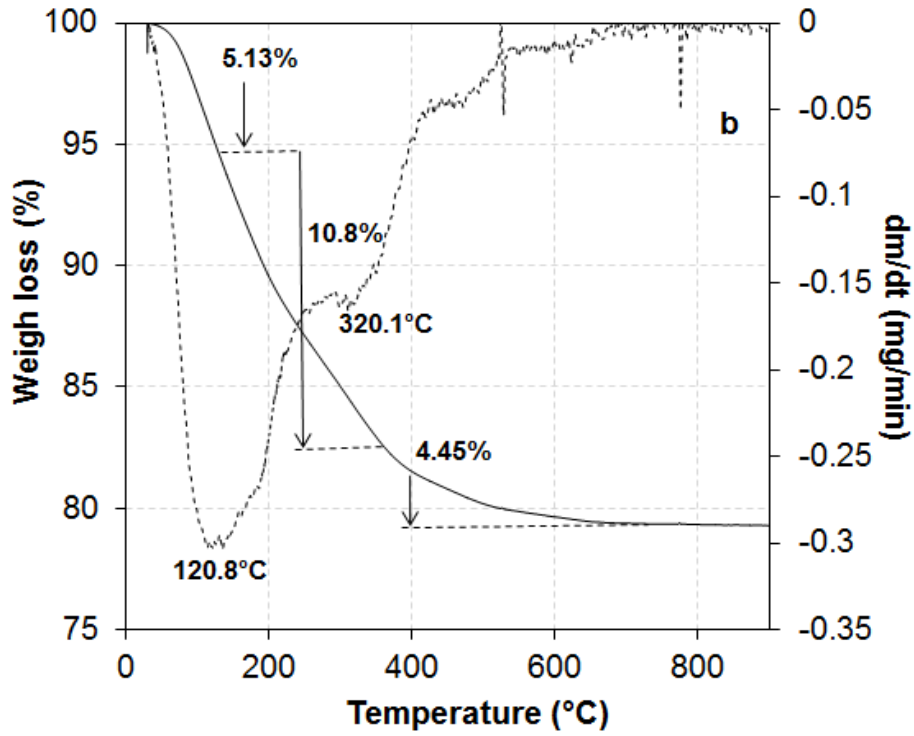


Figure III.16. TG –DTG profiles for a) FeLDH and b) Fe/FeLDH

TEM study was performed to remark the micromorphology characteristics of the iron substituted clay before and after reconstruction process.

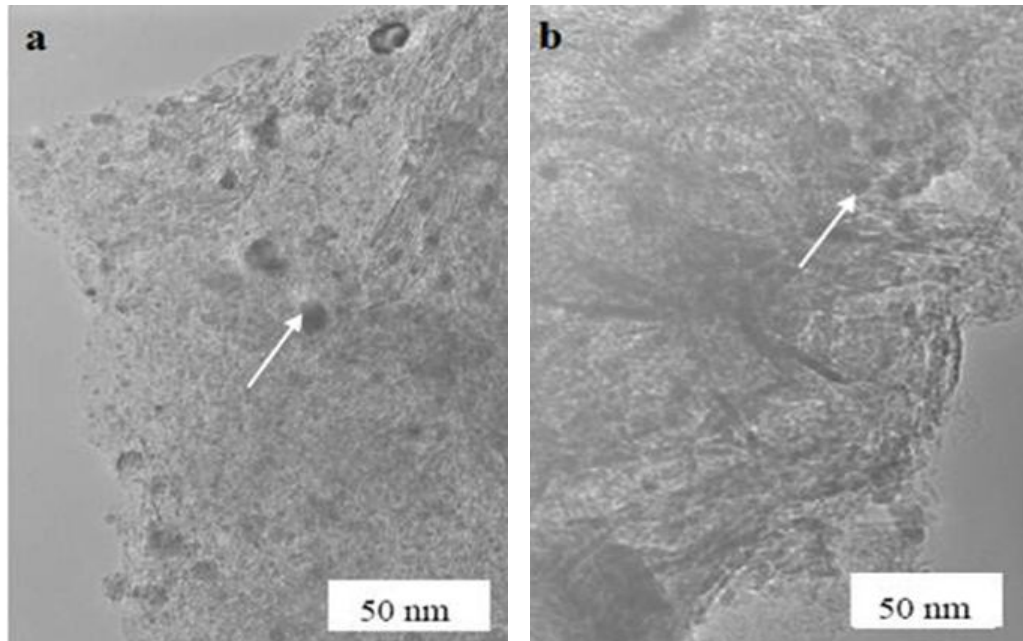


Figure III.17. TEM micrographs of reconstructed clays a) Fe/FeLDH1; b) Fe/FeLDH2

If TEM micrograph of as-synthesized FeLDH show the characteristic lamellar structure of LDH with particle intensely agglomerated, nearly hexagonal in shape, with the particle size equal to 110 nm (Carja et al., 2009), TEM images for the Fe/FeLDH and Fe/FeLDH2 (Figure III.17a and III.17b) reveal nanoparticles of iron oxide much smaller and well dispersed on the larger particles of FeLDH. Their size is equal to 9 nm for Fe/FeLDH1 and 12 nm for Fe/FeLDH2 respectively.

IV. PHOTOCATALYTIC APPLICATIONS OF LDHS, ME/LDHs and M_xO_y /LDHs NANOSTRUCTURED ASSEMBLIES

IV.1. Hydrogen generation from water splitting process

Herein we present, for the first time, Au nanoparticles loaded on mesoporous LDHs (Au/LDHs) as new plasmonic photocatalysts for H₂ production from water–methanol mixtures by using solar light, at room temperature. LDHs with a large compositional diversity can be designed by altering the nature of the metal cations in the anionic clay layers. We chose ZnAlLDH and ZnCeAlLDH as clay supports containing cations of the clay layers Zn²⁺/Al³⁺ and Zn²⁺/Ce³⁺/Al³⁺, respectively. The cations of LDH layers are distributed orderly in the LDH matrix as MeO₆ octahedra. Thus, the above LDH composition is defined by a specific arrangement of ZnO₆, AlO₆ and CeO₆ octahedra that are able to develop semiconductor features and the particular interactions with plasmonic gold.

For testing the photocatalytic properties of the derived materials type Au/ZnAlLDH and Au/ZnCeAlLDH, the samples were analyzed by the UV-Vis spectroscopy, techniques that allow the identification of certain chemical species that absorb light in the ultraviolet-visible range. The UV-Vis spectra for the samples Au/ZnAlLDH, Au/ZnCeAlLDH and derived mixed oxides is shown in figure IV.2.

All spectra show a strong and broad band at around 550 nm attributed to the SPR band of well dispersed Au NPs which originates from the intraband excitation of electrons in the outer orbital (6sp) of the Au species. The SPR peak is slightly red-shifted (by ~20 nm) for the cerium containing samples.

Furthermore, Au/ZnAILDH750 and Au/ZnCeAILDH750 show much stronger absorption intensity although the amounts of Au of the calcined and reconstructed anionic clays are almost coincident (see Table III.1).

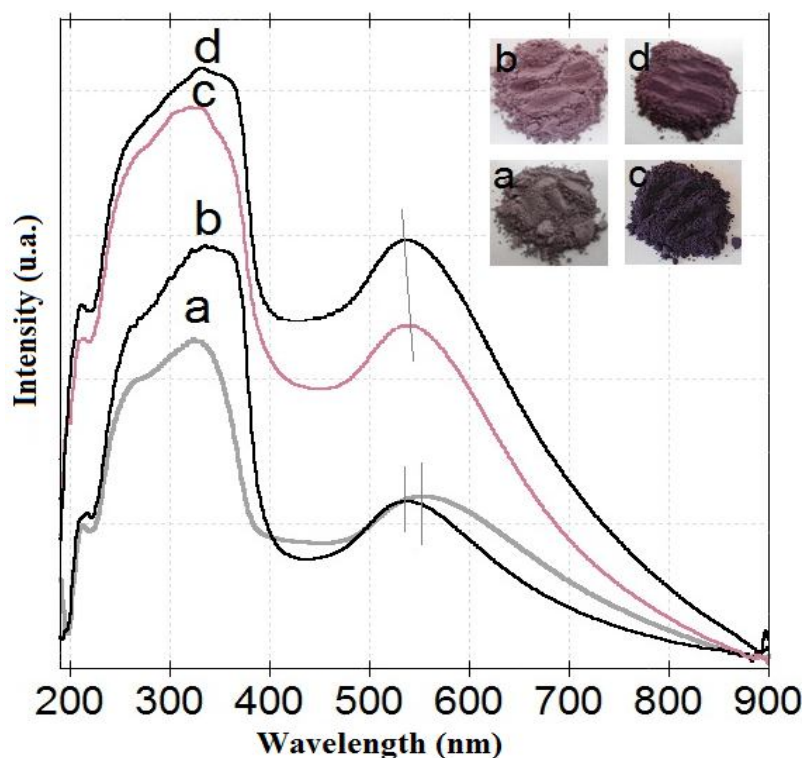


Figure IV.2. The UV-Vis absorption spectra for: a) Au/ZnAILDH; b) Au/ZnCeAILDH; c) Au/ZnAILDH750; d) Au/ZnCeAILDH750.

This assumption is in concordance with the literatures data reported for Au/TiO₂ and Au/CeO₂ and was interpreted considering that the intensity of light absorption due to SPR of Au is strongly affected by the size of the Au nanoparticles. Moreover, as indicated in the inset of figure IV.2, the tested photocatalytic powders are colored in different wine-red intensities which are consistent with the specific absorption characteristics of Au nanoparticles.

A relevant property in determining the photocatalytic activity is the configuration of the semiconductor energy band (E_g). The determination of energy band is a fundamental aspect in synthesis and photocatalysts design. The band gap energy configuration defines the incident photon absorption, the photo-oxidation of electron pair and holes, migrating charge carriers and redox capacities of electrons and holes in the excited state.

Figure IV.3 illustrates the graphs expressing the dependence of $(\alpha E_{\text{foton}})^2 - E_{\text{foton}}$.

The values of band gap energy were 3.21 eV for Au/ZnAILDH, respectively 3.16 eV for Au/ZnCeAILDH, values that are similar to the literature data reported for ZnO and gold nanoparticles deposited on Ce-Al-O mixed oxide. The thermal treatment changes the values of

band gap energy for this materials used as photocatalysts. After the calcination process at 750°C, the values of band gap energy are significantly lower and equal with 1.72 eV for Au/ZnAlLDH750 and 1.64 eV for Au/ZnCeAlLDH750.

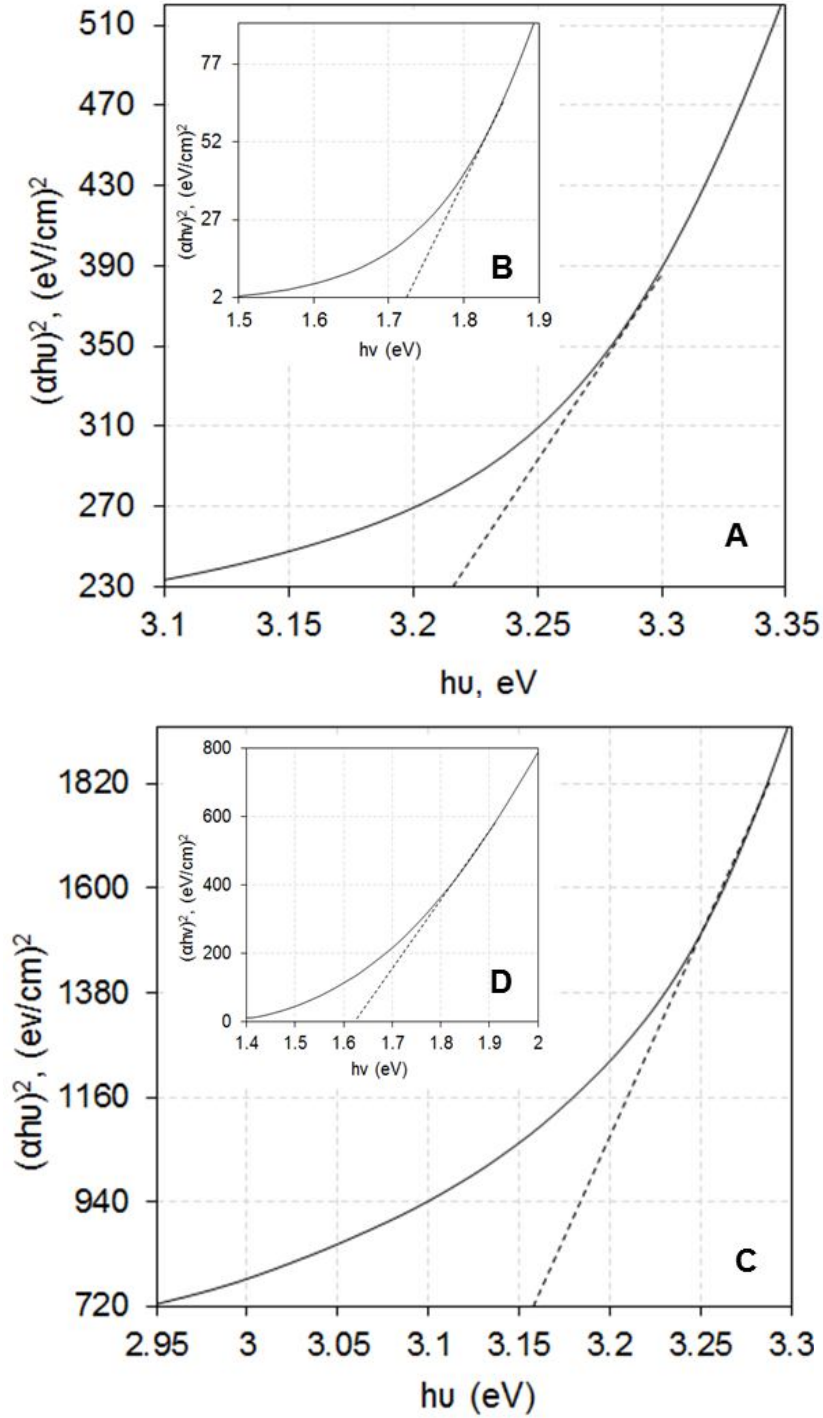


Figure IV.3. $(\alpha E_{\text{foton}})^2 - E_{\text{foton}}$ graphs for A) Au/ZnAlLDH; B) Au/ZnAlLDH750; C) Au/ZnCeAlLDH; D) Au/ZnCeAlLDH750.

Figure IV.4 shows the time course of H₂ evolution from water–methanol mixtures using Au/LDHs and Au/LDH750, under solar irradiation, at room temperature. The evolved H₂ amount was monitored at 1 h intervals and no H₂ was detected without irradiation. Moreover, Au-free samples (only ZnAILDH, ZnCeAILDH and the solid mixtures formed by calcination at 750°C) were unable to generate detectable amounts of H₂. Almost linear correlations are observed between the amount of evolved hydrogen and the irradiation time. The order of the catalytic activity is: Au/ZnCeAILDH > Au/ZnAILDH > Au/ZnCeAILDH750 > Au/ZnAILDH750 suggesting that the presence of Ce in the LDH promotes the catalytic activity of the material though calcination plays an adverse role with regard to the photocatalytic activity.

After irradiation for 7 h, the H₂ production reaches up to 127 μmol for Au/ZnAlCeLDH and 94 μmol for Au/ZnAILDH.

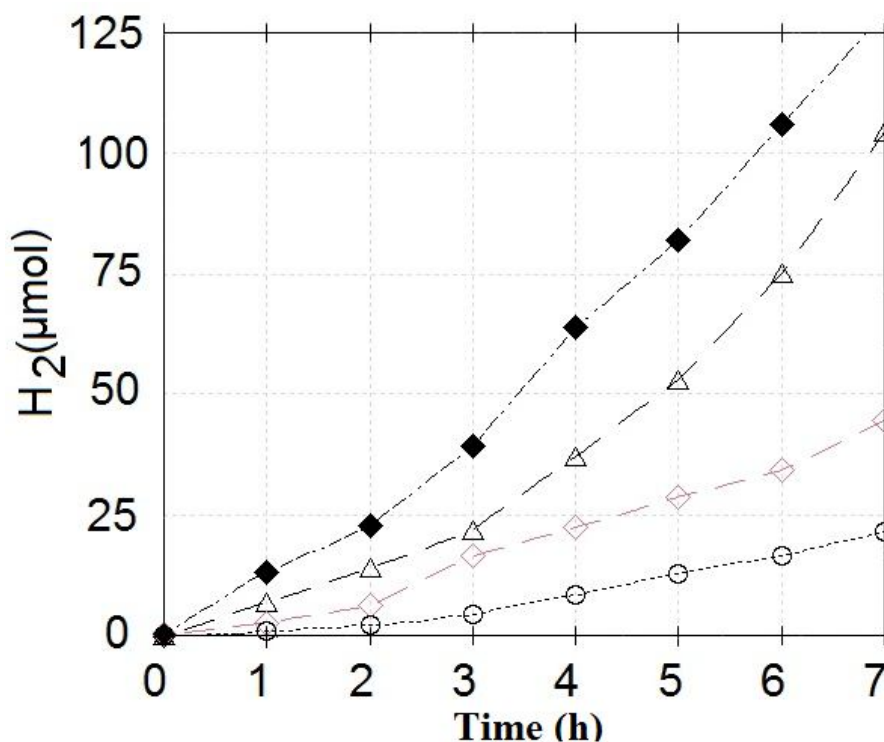


Figure IV.4. Temporal evolution of H₂ from water-methanol mixtures (80/20%) using Au/LDHs and Au/LDH750 photocatalysts, under solar light and room temperatures; (♦) Au/ZnCeAILDH; (Δ) Au/ZnAILDH; (○) Au/ZnAILDH750; (◇) Au/ZnCeAILDH750.

For the catalysts obtained after calcination at 750°C, the production of H₂ was significantly lower, decreasing in comparison with the uncalcined samples to 47 μmol for Au/ZnCeAILDH750 and 23 μmol for Au/ZnAILDH750. Calcination gave rise to a large increase in D_{Au} while the S_{Au} values strongly decreased (see Table III.1). Because all the

photocatalysts have almost similar values of Au content (equal to approximately 4%), the above results show that with the decrease of S_{Au} values, the efficiency of the photocatalyst for H_2 production from water–methanol mixtures under solar simulation also decreased.

On the other hand, so is $3.43\% \cdot 10^2 \text{ m}^2 \cdot \text{g}^{-1}$ for Au/ZnCeAILDH and slight increases in $3.97 \cdot 10^2 \text{ m}^2 \cdot \text{g}^{-1}$ for Au/ZnAILDH, though Au/ZnCeAILDH shows the superior activity for H_2 production than Au/ZnAILDH. Further, H_2 production of Au/ZnCeAILDH750 is higher than that of Au/ZnAILDH750, although these catalysts are defined by almost similar S_{Au} values. The photocatalysts were characterized after the water splitting process to observe their texture changes using scanning electron microscopy. Figure IV.7 presents the SEM images of the photocatalysts type layered double hydroxides LDHs.

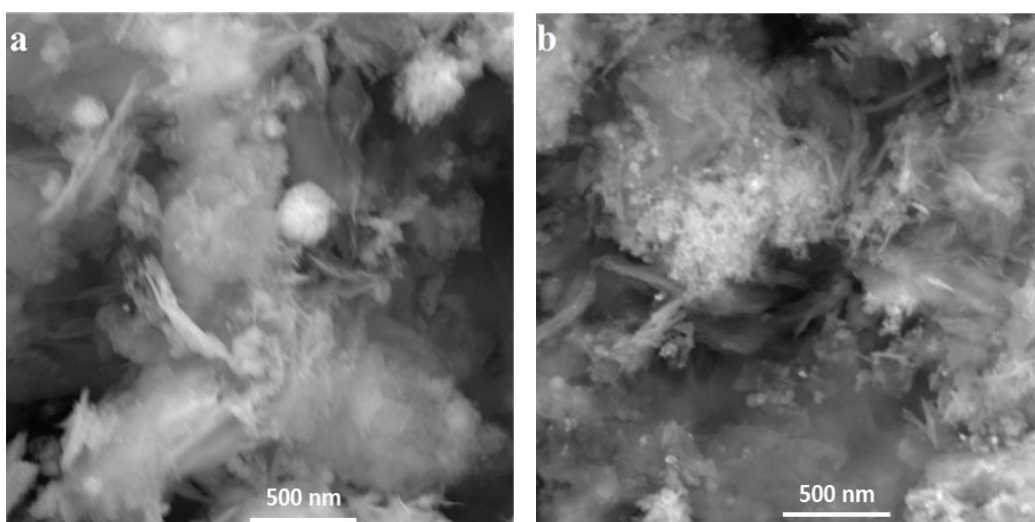


Figure IV.7. SEM images of derived materials: a) Au/ZnAILDH and b) Au/ZnCeAILDH after the water splitting process.

Methylene Blue degradation under visible light

Photocatalytic activity for all the samples was tested by degradation of dye molecules of Methylene Blue (MB). Photocatalysis study was carried out by using 25 mg of catalyst in 25 mL of solution containing Methylene Blue (MB) with an initial concentration of dyes equal to 40 mg/L. Prior to the catalytic experiments the aqueous solution with the dye and the catalyst were stirred in the dark for about 1h to establish the adsorption – desorption equilibrium, until the dye concentration remained constant. The weight of the catalyst was always maintained the same (1g/L). A 200 W xenon doped mercury lamp (Hamamatsu Lightningcure LC8), with a cutoff filter for visible light irradiation ($\lambda > 420 \text{ nm}$) was used as the light source for the photocatalytic reaction.

Figure IV.8 illustrates the temporal evolution of the spectral changes that take place during the photo degradation process of MB.

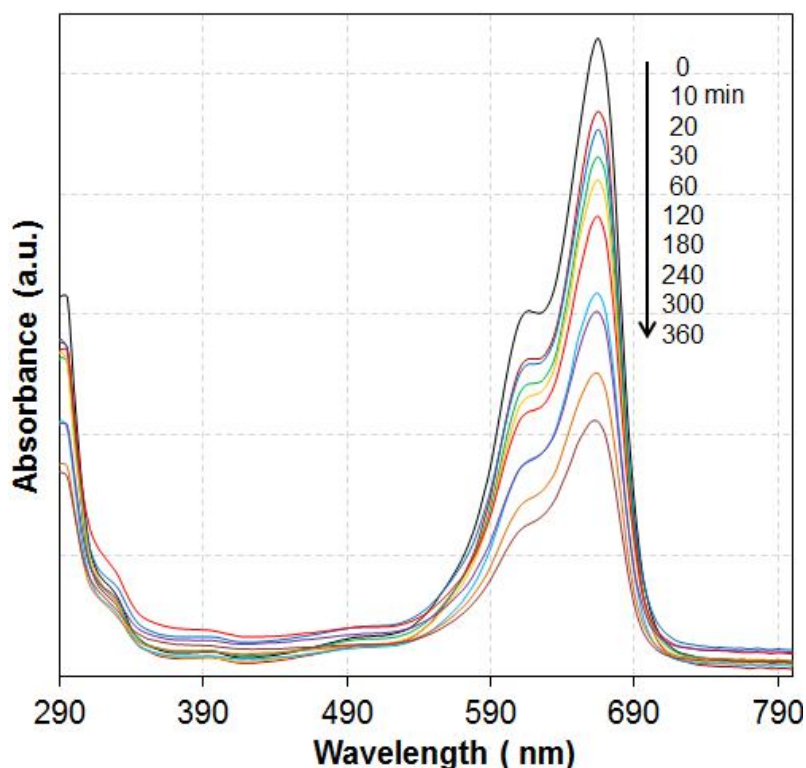


Figure IV.8. Temporal evolution of UV-Vis spectral changes taking place during the photodegradation of MB using Au/ZnCeAILDH2 photocatalyst.

The dye concentration was monitored by UV-Vis analysis by applying Beer-Lambert law. For the entire range of wavelength the photocatalytic efficiency of the reconstructed clays Au/ZnCeAILDH1 and Au/ZnCeAILDH2 and the derived solid solutions are compared in figure IV.9. Au/ZnCeAILDH2 shows the highest catalytic activity with almost 66% degradation of the dye after 6 h under visible irradiation, while in the same conditions Au/ZnCeAILDH1 degrades only 46% of the dye. The derived solid solutions displayed lower photocatalytic efficiency, thus the removal efficiency of MB apparently decrease by almost 6% for the calcined samples over the entire range of wavelength. For the parent clay ZnCeAILDH1 and ZnCeAILDH2, the MB degradation efficiency is 10% and 16% respectively.

The degradation of MB dye likewise under the same conditions was studied by using the dye solution without the catalysts as reference sample. It was found that any degradation of the dye take place during the photodegradation process using visible light irradiation.

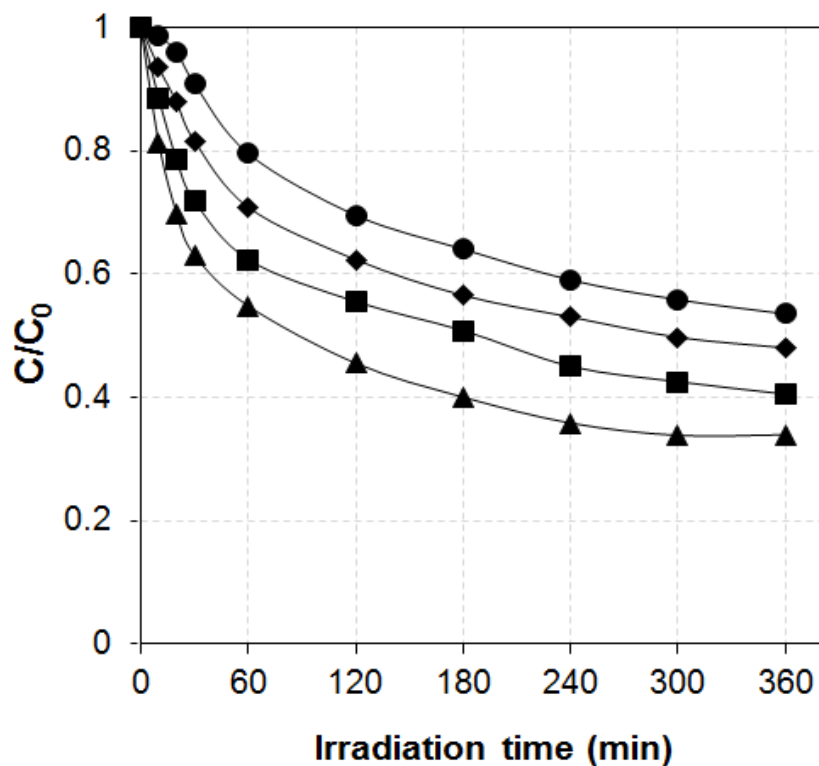


Figure IV.9. Comparison of the photocatalytic efficiency of the catalysts during the photodegradation process of MB over the entire range of wavelength.

(●) Au/ZnCeAILDH1 600; (◆) Au/ZnCeAILDH1; (■) Au/ZnCeAILDH2 600;
(▲) Au/ZnCeAILDH2;

IV.2. Photocatalytic activity: tests for the degradation process of some industrial dyes

The LDHs materials present a special property that is “so-called” structural “memory effect”. During the calcinations process at moderate temperature between 300 and 600°C, the layered structure can be destroyed and the clay is decomposed into mixed oxides with high specific surface area and homogeneous dispersion of metal cations. These calcined layered double hydroxides have the capability to restore the original layered structure by treatment with aqueous solutions containing anions. Considering their important property, this work has been focused to synthesize new nanostructured photo-responsive catalytic formulations of FeLDH clay reconstructed in FeSO₄ aqueous solutions.

The photocatalytic activity of both as-synthesized FeLDH and reconstructed clays Fe/FeLDH was testing for degrading two industrial dyes from aqueous solution. The dyes, Drimaren Red and Nylosan Navy (denoted as DR and Nyl) were offered by Clariant Product, Switzerland. Photocatalysis tests were carried out by using 0.1g of catalyst in 150 ml aqueous solution with an initial concentration of the dyes equal to 0.15 g/L. Before starting the

catalytic experiments the aqueous solution of the dyes and the catalyst were stirred in the dark for 1h, to establish the adsorption– desorption equilibrium, until the dye concentration remained constant.

As irradiation source was used a UV Pen – Ray power supply placed in a quartz tube with the intensity of 4400 mW/cm². During the irradiation, at different time intervals, samples of the suspension were collected, the catalyst was removed by centrifugation and then monitored by UV–Vis analysis following the absorbance (A) at 277 nm and 575 nm characteristic to DR and Nyl respectively. Also was made a photocatalytic reaction, following the same procedure, without the catalyst.

Regarding photocatalytic activity, important information about the photo-responsive properties of the materials can be supplied by the optical spectrum. The optical absorption of the original clay and reconstructed samples in the UV – Vis region is shown in figure IV.10.

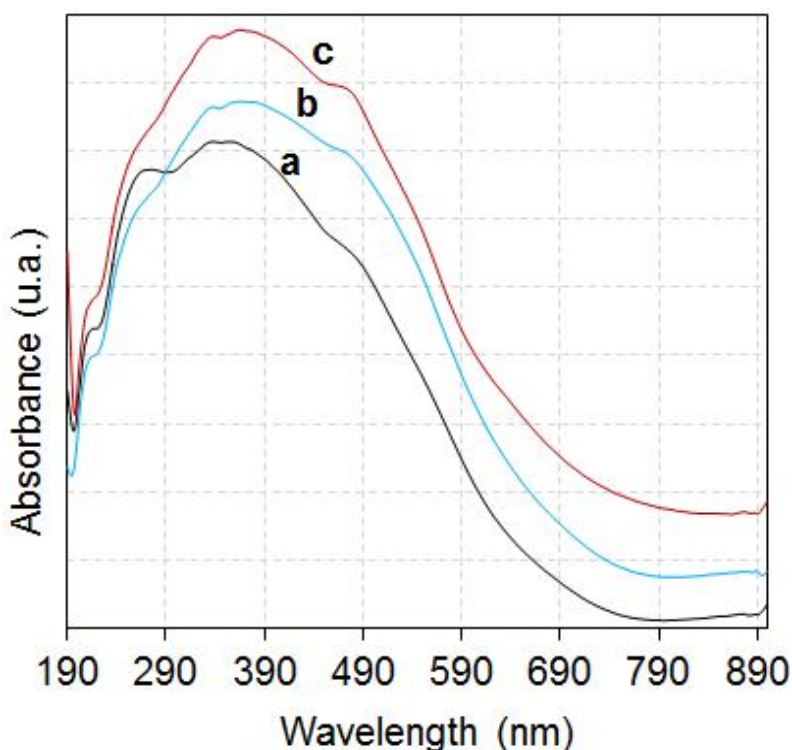


Figure IV.10. The UV–Vis absorption spectra of: a) FeLDH; b) Fe/FeLDH1; c) Fe/FeLDH2.

The absorption spectra of FeLDH show absorption bands at around 270 nm and between 300 and 450 nm, related to charge transfer excitations occurring in the MeO₆ octahedra of layered structure. The band around 450 – 560 nm indicate the occurrence of Fe³⁺ as large particles (Bordiga et al., 1996, Carja et al., 2011). For the reconstructed clays, the absorption band nearly 400 nm appears due to the d-d transition of Fe³⁺. The absorbance at wavelength $\lambda > 500$ nm is due to d-d transition of the Fe₂O₃ particles formed on the surface of the iron layered double hydroxides (Parida et al., 2011).

The photocatalytic activity of the layered double hydroxides before and after the reconstruction process was tested for the degradation of two industrial dyes Drimaren Red (DR) and Nylosan Navy (Nyl) from aqueous solution under UV light irradiation.

Figure IV.11 illustrates the temporal evolution of the spectral changes that take place during the photo degradation process of DR. The degradation rate of DR with LDHs used as photocatalyst is shown in figure IV.12.

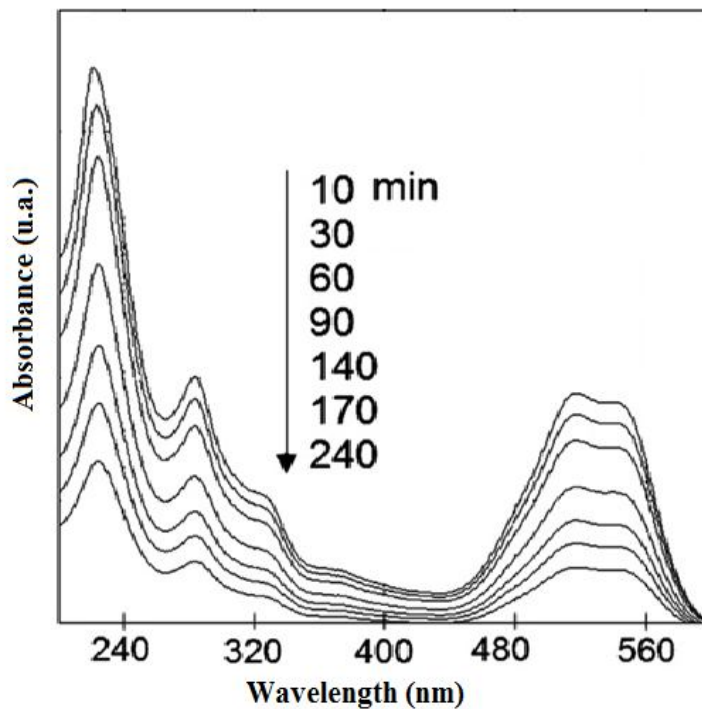


Figure IV.11. Temporal evolution of UV spectral changes taking place during the photodegradation of DR using Fe/FeLDH2 photocatalyst.

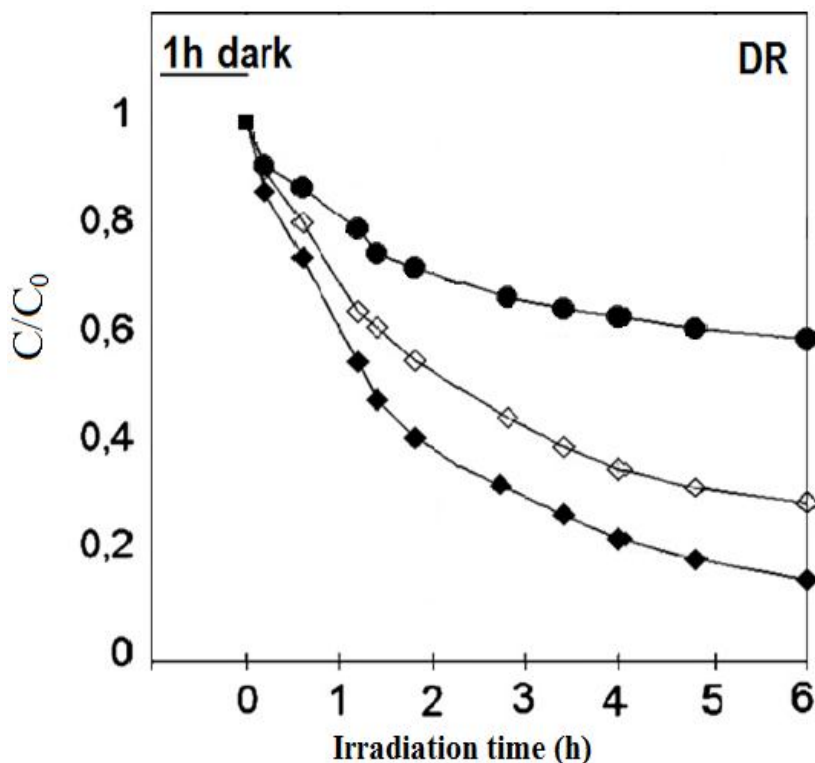


Figure IV.12. Degradation of DR under UV – light using as-synthesized and reconstructed clays as catalysts; (●) FeLDH; (◇) Fe/FeLDH1; (◆) Fe/FeLDH2.

After 6 h under irradiation can be identified a catalytic degradation of DR reached nearly 86% when is used as catalyst Fe/FeLDH2 and 72% when the catalyst is Fe/FeLDH1. For the as-synthesized clay FeLDH almost 38% of the aqueous solution containing the dye was degraded after 6 h under irradiation.

In case of Nyl, figure IV.13 presents the temporal profile of the spectral changes taking place during the photodegradation process.

Figure IV.14 shows that the degradation of the dye, after 6 h under irradiation, for Fe/FeLDH2 is 79%, whereas for Fe/FeLDH1 the photocatalytic degradation reached nearly 70%. For FeLDH less than 40% of the dye is degraded after 6 h under UV light irradiation.

The degradation of both dyes DR and Nyl under the same conditions were studied by using the dye solution without the catalysts as a reference sample. It was found that any degradation of the dye takes place during the photodegradation process.

This result indicates that the catalytic performances of the reconstructed clays Fe/FeLDH1 and Fe/FeLDH2 could be altered not only by the nano-sized oxidized iron on the clay surface, but also by the specific composition of the as-synthesized clay and the synthesis conditions.

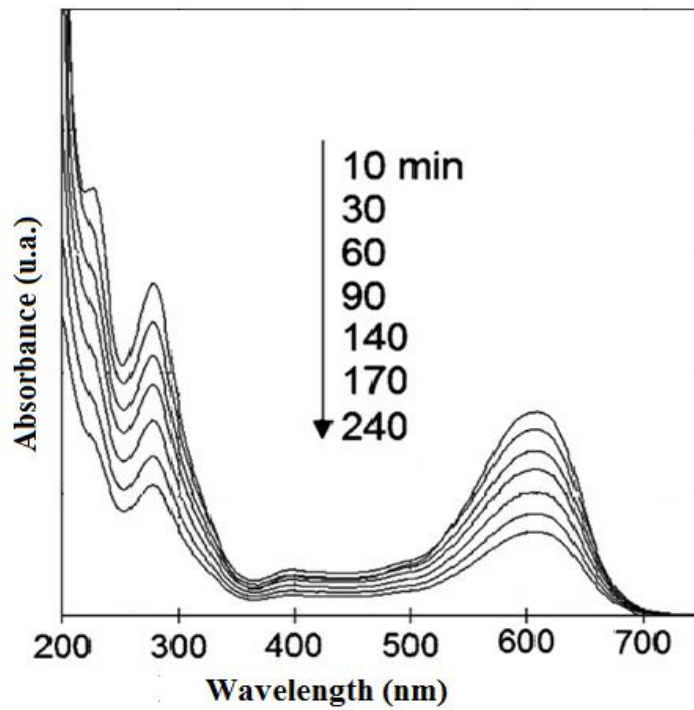


Figure IV.13. Temporal evolution of the UV spectral changes taking place during the photodegradation of Nyl on Fe/FeLDH2 photocatalyst

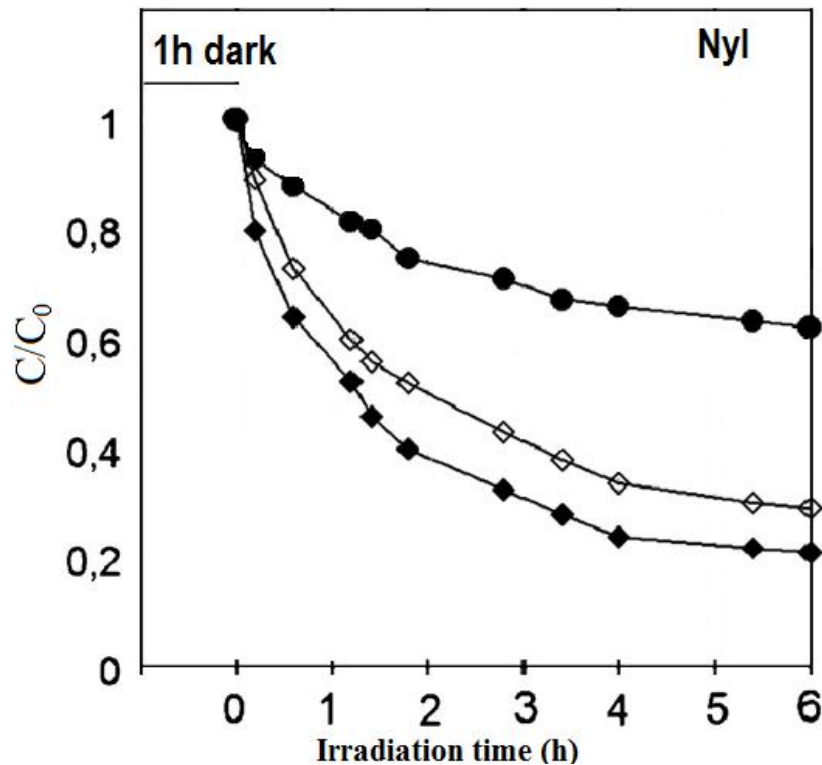


Figure IV. 14. Degradation of Nyl under UV – light irradiation using catalysts before and after reconstruction process; (●) FeLDH; (◇) Fe/FeLDH1; (◆) Fe/FeLDH2.

MAIN CONCLUSIONS

- New knowledge was obtained regarding the tailored structural reconstruction of layered double hydroxides in Me^+X^- aqueous solutions.
- The different nature of the anions from the LDHs interlayer can be tailored as a function of the nature of X^- from Me^+X^- aqueous solution.
- XRD, XPS and TEM analysis demonstrated that during the reconstruction process in Au^+X^{3-} aqueous solution NPs of Au were organized as well dispersed NPs on the surface of the LDHs in Au/LDHs nanostructures. Further, nanoparticles of Fe_2O_3 are highly dispersed on LDH surface after the reconstruction process in $\text{Fe}^{y+}\text{X}^{3-}$.
- The parameters used during the reconstruction process, like temperature, stirring rate, aging time, might be used to tailor the size and dispersity of MeNPs in Au/LDHs and Fe_2O_3 /LDHs nanostructures.
- The results show that the studied Au/LDHs nanostructures are active as nanostructured catalysts for the hydrogen generation from water, using solar radiation at room temperature, with Au/LDHs photocatalysts.
- The photocatalytic results revealed that nanostructures precursor type LDHs are more active than derived mixed oxides resulting after the calcination process; this decrease of the photocatalytic activity is due to the increase of the efficiency nanoparticles size of the matrix surface.
- The presence of cerium in the LDH layers favors the electron injection from nanoparticles of Au to LDH semiconductor leading to a larger population of positive Au ($^+$ or $^{3+}$) on the catalyst surface and enhances the photocatalytic performances.
- Fe/LDH nanoassemblies are active catalysts in the photocatalytic degradation process of some industrial dyes Nylosan Navy and Drimaren RED (offered by the CLARINTE PRODUCKT Company from Switzerland).
- The results about the photocatalytic performance of anionic clay type Fe/FeLDH have shown that these materials exhibit better photocatalytic activity compared to the LDHs precursor, Fe/FeLDH2 photocatalyst degrading almost 80% of the total amount of the dye from aqueous solutions, after 6 h of UV irradiation.

References

- Forano C., Costantino U., Prévot V., Taviot Gueho C., (2013), Layered Double Hydroxides (LDH), in Bergaya F., Lagaly G., *Handbook of Clay Science, Second Edition, Part. A Fundamentals*, **5**, 745–782, Elsevier Ltd.
- Bouariu S., Dartu L., Carja G., Silver-layered double hydroxides self-assemblies, *J Therm Anal Calorim*, **111**, 1263–1271.
- Carja G., Dartu L., Okada K., Fortunato E., (2013), Nanoparticles of copper oxide on layered double hydroxides and the derived solid solutions as wide spectrum active nanophotocatalysts, *Chem. Eng. J*, **222**, 60–66.
- Carja G., Husanu E., Gherasim C., Iovu H., (2011), Layered double hydroxides reconstructed in NiSO₄ aqueous solution as highly efficient photocatalysts for degrading two industrial dyes, *Appl Catal B-Environ.*, **107**, 253–259.
- Ballarin B., Mignani A., Scavetta E., Giorgetti M., Tonelli D., Boanini E., Mousty C., Prevot V., (2012), Synthesis route to supported gold nanoparticle layered double hydroxides as efficient catalysts in the electrooxidation of methanol, *Langmuir*, **28** (42), 15065–15074.
- Carja G., Kameshima Y., Nakajima A., Dranca C., Okada K., (2009), Nanosized silver–anionic clay matrix as nanostructured ensembles with antimicrobial activity, *Int. J. Antimicrob. Ag.* **34**, 534–539.
- Carja G., Birsanu M., Okada K., Garcia H., (2013), Composite plasmonic gold/layered double hydroxides and derived mixed oxides as novel photocatalysts for hydrogen generation under solar irradiation, *J. Mater. Chem. A*, **1**, 9092-9098.
- Birsanu M., Puscasu M., Gherasim C., Carja G., (2013), Highly efficient room temperature degradation of two industrial dyes using hydrotalcite-like anionic clays and their derived mixed oxides as photocatalysts, *Environ. Eng. Manag. J.*, **12**, 1535-1540.
- Gomes Silva C., Bouizi Y., Fornés V., García H., (2009) Layered double hydroxides as highly efficient photocatalysts for visible light oxygen generation from water, *J. Am. Chem. Soc.*, **131**, 13833-13839.